

文章编号: 0258-7106(2015)02-0289-20

Doi: 10.16111/j.0258-7106.2015.02.006

黑龙江省铜山铜矿床英云闪长岩锆石 U-Pb 年龄及地球化学特征^{*}

刘军¹, 周振华¹, 何哲峰^{2,3}, 欧阳荷根¹

(1 中国地质科学院矿产资源研究所 国土资源部成矿作用与资源评价重点实验室, 北京 100037;

2 中国地质博物馆, 北京 100034; 3 中国地质大学, 北京 100083)

摘要 铜山矿床是位于大兴安岭北段多宝山矿田中的一个大型铜矿床。文章对该矿区含矿英云闪长岩进行了详细的 LA-MC-ICP-MS 锆石 U-Pb 定年、主量元素、微量元素及同位素地球化学研究。锆石 U-Pb 定年结果表明, 英云闪长岩侵位于(461 ± 1) Ma。岩石显示埃达克质岩的地球化学特征, 具有高 $w(\text{SiO}_2)$ (62.5% ~ 64.53%) 和 $w(\text{Al}_2\text{O}_3)$ (14.77% ~ 17.7%), 高 $w(\text{Sr})$ (394×10^{-6} ~ 804×10^{-6}), 低 $w(\text{Y})$ (7.78×10^{-6} ~ 10.3×10^{-6}) 和 $w(\text{Yb})$ (0.8×10^{-6} ~ 1.04×10^{-6}), 轻稀土元素富集, 重稀土元素亏损, 无明显 Eu 异常。锆石 $\epsilon_{\text{Hf}}(t)$ 值介于 11.6 ~ 13.5。金属硫化物的 $\delta^{34}\text{S}$ 值为 -1.3‰ ~ -0.4‰, $^{206}\text{Pb}/^{204}\text{Pb}$ 、 $^{207}\text{Pb}/^{204}\text{Pb}$ 和 $^{208}\text{Pb}/^{204}\text{Pb}$ 值分别为 17.591 ~ 18.453、15.449 ~ 15.551 和 37.280 ~ 37.999。这些特征表明, 铜山矿床英云闪长岩形成于大陆边缘弧环境, 是加厚下地壳部分熔融的产物。成矿物质主要来自于英云闪长岩及多宝山组火山岩。

关键词 地球化学; 锆石 U-Pb 定年; Hf 同位素; 硫铅同位素; 英云闪长岩; 铜山矿床

中图分类号: P618.41; P597

文献标志码: A

Zircon U-Pb dating and geochemistry of ore-bearing tonalite in Tongshan copper deposit, Heilongjiang Province

LIU Jun¹, ZHOU ZhenHua¹, HE ZheFeng^{2,3} and OUYANG HeGen¹

(1 MLR Key Laboratory of Metallogeny and Mineral Assessment, Institute of Mineral Resources, Chinese Academy of Geological Sciences, Beijing 100037, China; 2 Geological Museum of China, Beijing 100034, China; 3 China University of Geosciences, Beijing 100083, China)

Abstract

The Tongshan deposit is a large copper deposit located in the Duobaoshan orefield within the northern Da Hinggan Mountains. This paper reports LA-MC-ICP-MS zircon U-Pb age, major and trace elements, and isotopic geochemistry of the ore-related tonalite in the Tongshan deposit. LA-MC-ICP-MS zircon U-Pb dating yielded the crystallization age of (461 ± 1) Ma for the tonalite. The tonalite shows characteristics of adakitic affinity, i.e., high SiO_2 (62.5% ~ 64.53%), Al_2O_3 (14.77% ~ 17.7%) and Sr (394×10^{-6} ~ 804×10^{-6}), low Y (7.78×10^{-6} ~ 10.3×10^{-6}) and Yb (0.8×10^{-6} ~ 1.04×10^{-6}), slight Eu anomalies, rich light rare-earth elements and depleted heavy rare-earth elements. The zircon Hf isotope analysis shows $\epsilon_{\text{Hf}}(t)$ values of 11.6 to 13.5. $\delta^{34}\text{S}$ values of sulfides are between -1.3‰ and -0.4‰, similar to data associated with mag-

* 本文得到中国地质调查局地质调查项目(12120113093600)和国家自然科学基金项目(41172081)联合资助

第一作者简介 刘军, 男, 1983 年生, 博士, 矿床学专业。Email: junliu@yeah.net

收稿日期 2014-07-26; 改回日期 2014-10-01。张绮玲编辑。

matic-hydrothermal systems. $^{206}\text{Pb}/^{204}\text{Pb}$, $^{207}\text{Pb}/^{204}\text{Pb}$ and $^{208}\text{Pb}/^{204}\text{Pb}$ ratios vary from 17.591 to 18.453, 15.449 to 15.551, and 37.280 to 37.999, respectively. The tonalite was formed in a continental marginal arc setting, and originated from partial melting of the thickened lower crust. The ore-forming materials were derived from the volcanic rocks of the Duobaoshan Formation and tonalite.

Key words: geochemistry, zircon U-Pb dating, Hf isotope, S-Pb isotope, tonalite, Tongshan deposit

多宝山斑岩型铜钼矿田位于大兴安岭北段, 主要由多宝山大型斑岩铜(钼)矿床、铜山大型斑岩铜矿床、三矿沟小型矽卡岩铁铜矿床、关鸟河小型矽卡岩白钨矿床及小多宝山、跃进、育宝山铁铜矿点等组成, 是中亚造山带东段最重要的斑岩型铜(钼)矿床产出地区(杜琦等, 1988; 韩振新等, 2004; 武广等, 2009; Liu et al., 2012)。近年来, 区域上又陆续发现了小泥鳅河金矿床、三道湾子金碲矿床、争光金锌矿床、铜山金矿床、上马厂金矿床等一批金银钼锑矿床或矿化点(谭成印等, 2010), 进一步拓展了区域找矿方向。前人对多宝山矿床开展了矿床地质、成岩成矿年代学、成矿流体演化、同位素地球化学等方面的研究(杜琦等, 1988; 刘弛等, 1995; 赵元艺等, 1995; 赵一鸣等, 1997a; Ge et al., 2007; 王喜臣等, 2007; 刘军等, 2010; Liu et al., 2012; 向安平等, 2012; Zeng et al., 2014), 但对矿田内铜山矿床的研究相对薄弱。铜山矿床位于多宝山矿床东南 4 km 处, 是矿田内第二大铜矿床, 已探明铜金属量 90.6 万吨, 平均品位 0.48%。目前对铜山矿床的研究工作主要集中在矿床地质和成矿流体演化方面(杜琦等, 1988; 王喜臣等, 2007; 武广等, 2009; 付艳丽, 2010; Wang et al., 2012), 而对矿床成因及成矿背景方面的研究仍显薄弱。为此, 本文以铜山矿区与成矿关系密切的英云闪长岩体为主要研究对象, 通过系统的锆石 U-Pb 定年、岩石主量元素和微量元素、稀土元素及 Hf-S-Pb 同位素地球化学研究, 分析了该岩体的成因及其形成的地球动力学背景, 讨论了铜山矿床的成矿机制。

1 区域地质

多宝山铜钼矿田位于兴蒙造山带北东段, 地处嫩江断裂北西侧的兴安地块内(图 1a)。矿田内出露地层主要为奥陶系铜山组和多宝山组, 其次为志留系、泥盆系和白垩系(图 1b)。铜山组以沉积岩为主夹少量火山碎屑岩, 岩性为凝灰砂岩、粉砂岩、砂砾岩、凝灰岩及结晶灰岩; 多宝山组是一套滨海-浅海

相的火山熔岩、火山碎屑岩和碎屑火山沉积岩组合, 其中遍布矿区的主体岩石为安山岩、玄武岩; 志留系岩性为砂岩、粉砂岩、砂砾岩、板岩, 局部夹中基性火山岩; 泥盆系岩性为砂岩、粉砂岩、泥质板岩、板岩夹灰岩透镜体、安山岩、英安岩及凝灰熔岩和细碧岩等; 白垩系为一套陆相含煤建造(杜琦等, 1988; 韩振新等, 2004)。

区内发育多期岩浆岩, 包括早古生代、晚古生代和中生代花岗岩类(图 1b)。其中, 早古生代侵入岩为英云闪长岩、花岗闪长岩、花岗闪长斑岩和花岗斑岩, 其中花岗闪长岩的锆石 U-Pb 年龄为 (485 ± 8) Ma(Ge et al., 2007), 花岗闪长斑岩的锆石 U-Pb 年龄为 (477 ± 4) Ma(Zeng et al., 2014)。晚古生代花岗岩类包括花岗闪长岩、花岗闪长斑岩、石英闪长岩和斜长花岗岩, 其全岩 Rb-Sr 等时线年龄为 292 Ma 和 283 Ma(杜琦等, 1988); 花岗闪长岩的角闪石、黑云母和全岩同位素年龄(K-Ar 法、Rb-Sr 等时线法)为 226 ~ 310 Ma(赵一鸣等, 1997b)。中生代花岗岩类包括角闪花岗闪长岩、花岗闪长岩、钾长花岗岩和细晶闪长岩, 花岗闪长岩的锆石 U-Pb 年龄为 (177 ± 3) Ma 和 (176 ± 3) Ma(Ge et al., 2007)。

多宝山矿田受北西西向的三矿沟-多宝山-裸河构造带控制, 该构造带由北西向南东呈反“S”形弯曲, 由一系列褶皱和断裂组成, 长约 25 km(韩振新等, 2004; 李之彤等, 2008; 武广等, 2009; 刘军等, 2010)。

2 矿床地质

铜山矿床位于黑龙江省嫩江县北北东方向 160 km 处, 地理坐标: E125°48'30" ~ E125°50'30", N50°13'00" ~ N50°14'10"。矿区出露地层为奥陶系铜山组和多宝山组, 构成背斜构造(图 2、3)。侵入岩主要见英云闪长岩、花岗闪长岩、石英闪长岩、细晶闪长岩脉及闪长玢岩脉, 其中, 隐伏英云闪长岩体与铜矿化关系密切。花岗闪长岩体分布于矿区南部, 面积 0.02 km^2 , 呈北西向分布, 中间部位近圆形, 有分支

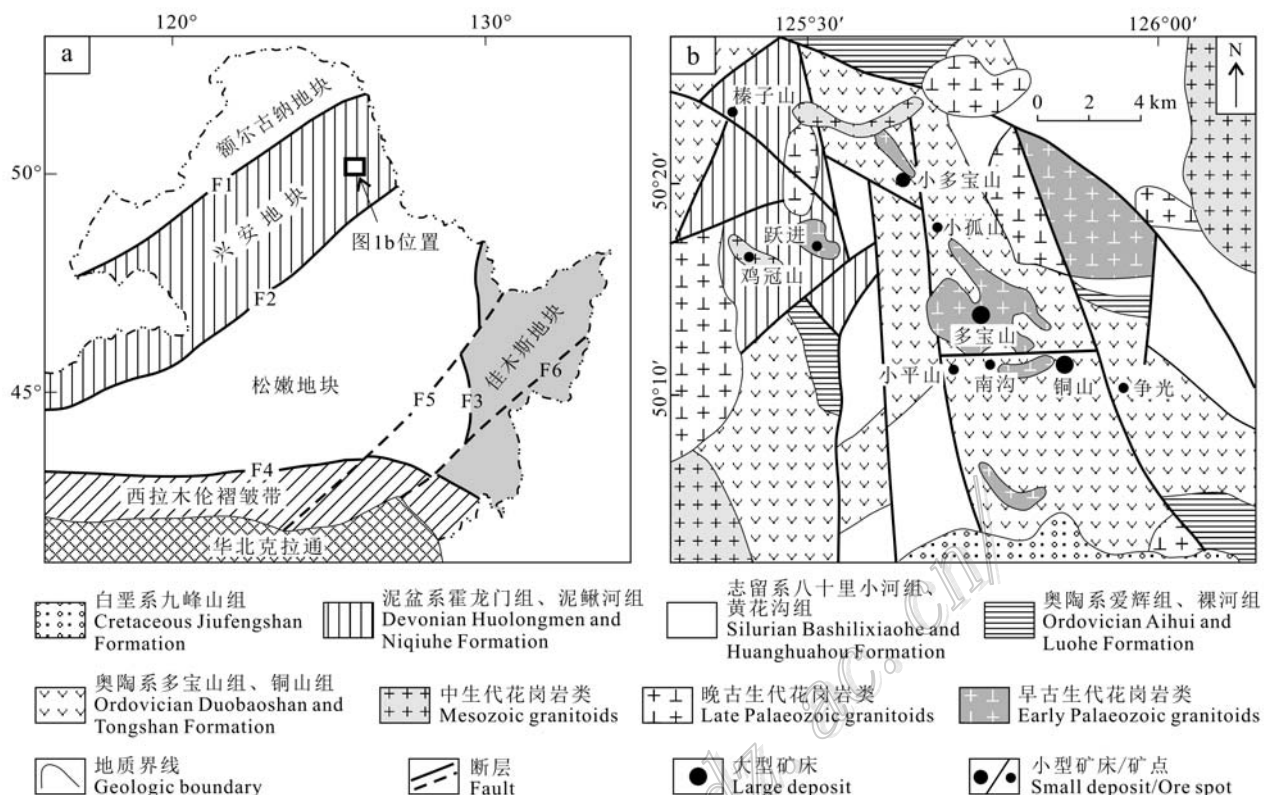


图1 铜山矿床大地构造位置(a, 据Ge et al., 2007资料改编)和区域地质简图(b, 据韩振新等, 2004资料修改)

F1—塔源-喜桂图断裂; F2—嫩江断裂; F3—牡丹江断裂; F4—西拉木伦-长春断裂; F5—依兰-伊通断裂; F6—敦化-密山断裂

Fig. 1 Sketch regional geological map of the Tongshan deposit in northwest Heilongjiang, showing geotectonic units

(a, modified after Ge et al., 2007) and locations of major deposits (b, modified after Han et al., 2004)

F1—Tayuan-Xiguitu fault; F2—Nenjiang fault; F3—Mudanjiang fault; F4—Xilamulun-Changchun fault; F5—Yilan-Yitong fault;

F6—Dunhua-Mishan fault

现象,捕捞体较多。岩石呈块状构造和花岗结构,由斜长石(50% ~ 55%)、石英(10% ~ 20%)、碱性长石(10% ~ 15%)、角闪石(10% ~ 15%)及黑云母(1% ~ 5%)组成;英云闪长岩体分布于矿区北西部、西部和中部,面积0.49 km²,呈北西向分布,接触面较规则,对围岩同化混染较强,几乎见不到捕捞体。岩石呈块状构造和花岗结构,主要矿物为斜长石(50% ~ 60%)、石英(15% ~ 25%)、黑云母(10% ~ 15%)及角闪石(5% ~ 10%)(图4a,b);石英闪长岩分布于矿区南西部,面积0.01 km²,呈岩墙状沿北东向展布,边缘较规则。岩石呈块状构造,中-细粒结构,主要由斜长石(70% ~ 80%)、石英(5% ~ 15%)、黑云母(1% ~ 5%)和角闪石(1% ~ 5%)组成(付艳丽,2010)。北西向反“S”型弧形构造带控制了蚀变和矿化的分布,近东西向的铜山断裂横切矿区,属成矿后断裂,为逆冲断层,控制长度大

于10 km,延伸到矿区外部,两侧岩性变化较大,切断岩体和地层。

矿床内已发现4个主矿体及其从属矿体群,其中以Ⅲ号矿体(群)规模最大。矿化类型以铜矿体为主,偶见钼矿体和铅锌矿体,铅锌矿体多出现于主矿体的上、下盘。Ⅰ号主矿体(群)赋存在铜山断层上盘多宝山组火山岩中,呈透镜状,矿体长750 m,水平厚度5 ~ 136 m,向下呈尖灭趋势,被铜山断层切断,矿体倾向218°,倾角75°,Cu平均品位0.61%。Ⅱ号主矿体(群)产在铜山断层上盘多宝山组火山岩中,矿体下部大半断失,呈透镜状,矿体长1800 m,最大水平厚度175 m,倾向210°,倾角60°,Cu平均品位0.51%。Ⅲ号主矿体(群)基本产于铜山断裂下盘的蚀变英云闪长岩中,少量位于蚀变火山岩及碎屑岩中,呈厚大透镜状,矿体长>1140 m,最大水平厚度156 m,延深>800 m,向下仍有膨大的趋势,目前工程

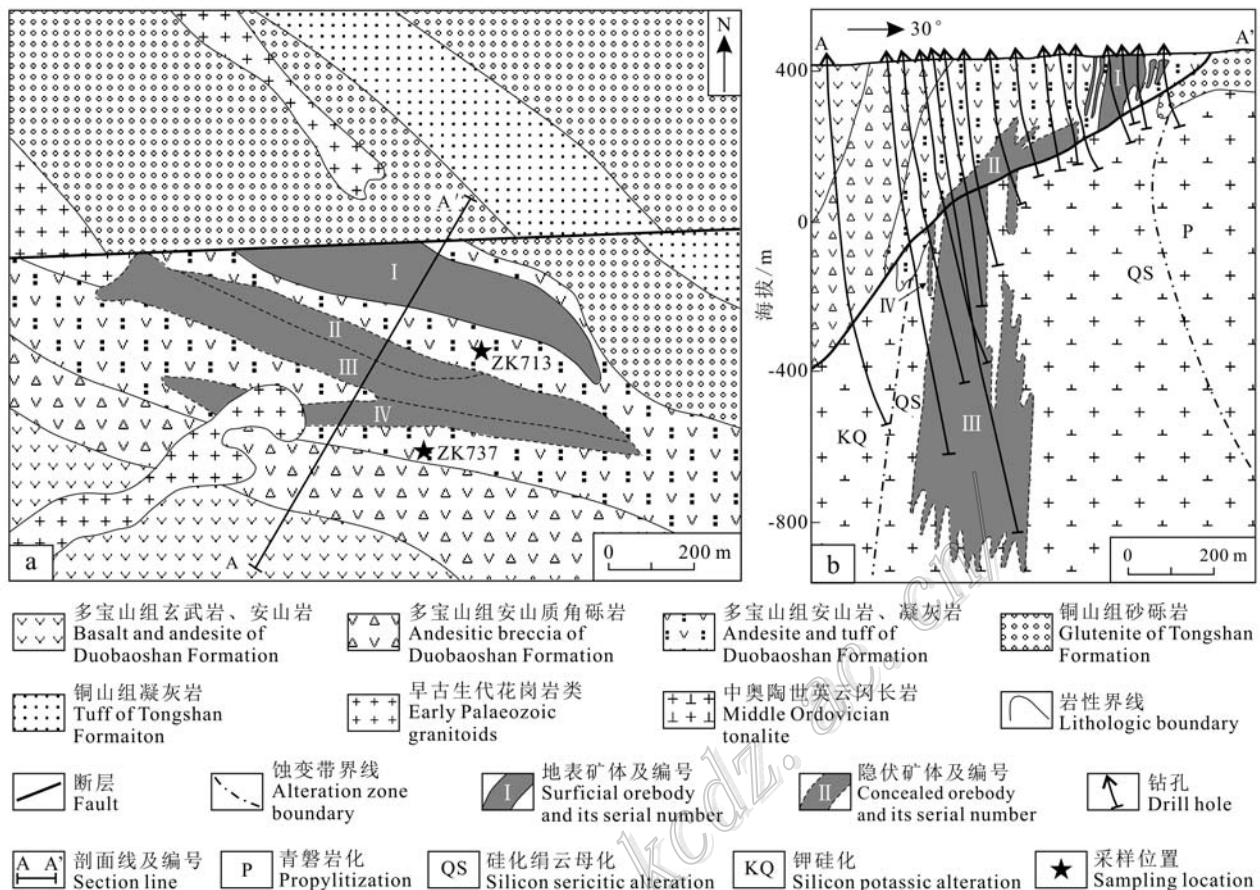


图 2 铜山矿床地质简图(a)和 1080 线剖面图(b)(据王喜臣等, 2007 修改)

Fig. 2 Simplified geological map (a) and geological cross section along exploration line 1080 (b) of the Tongshan deposit
(modified after Wang et al., 2007)

仍未穿透矿体, 矿体倾向 180°, 倾角 80°, Cu 平均品位 0.45%。Ⅳ号主矿体(群)位于Ⅲ号矿体(群)上盘附近, 呈条带状, 长 255 m, 水平厚度 9 m, 延深 144 m, 倾向 180°, 倾角 78°。矿石中金属矿物体积分数为 3%~7%, 主要为黄铜矿和黄铁矿(图 4c~f), 其次为蓝铜矿、斑铜矿、辉钼矿、赤铜矿、铜蓝、磁铁矿、镜铁矿、方铅矿、闪锌矿等。脉石矿物以石英、绢云母、绿泥石和碳酸盐为主, 其次为绿帘石、黑云母、钾长石、钠长石、高岭石、伊利石等。矿石构造主要为浸染状、细脉浸染状、细脉状及块状构造。矿石结构主要有斑状结构、粒状结构、交代结构、固溶体分离结构、受压力结构和重结晶结构等。围岩蚀变从南西向北东依次发育钾硅化、硅化绢云母化和青磐岩化 3 个蚀变带(图 2b)。青磐岩化带主要发育于远离矿体或接触带的围岩和岩体中, 矿物组合为绿帘石、绿泥石、钠长石、石英、绢云母、方解石和黄铁矿; 硅

化绢云母化带发育于矿体两侧数百米范围内, 与铜矿化关系密切; 钾硅化蚀变带发育于紧邻矿体的南西侧, 主要表现为钾长石-石英细脉和石英细网脉。上述 3 个蚀变带呈不对称分布, 向南西呈开放状态(王喜臣等, 2007)。

根据脉体穿插关系、矿石组构和矿物共生组合特征, 成矿过程划分为 3 个阶段: 早阶段主要矿物组合为石英、钾长石、黑云母、磁铁矿、黄铜矿、斑铜矿和微量的黄铁矿等, 金属矿物呈浸染状分布, 伴随钾长石化、硅化、黑云母化; 中阶段发育大量的石英、绢云母、绿帘石、黄铜矿、斑铜矿、黄铁矿及少量方铅矿和闪锌矿等, 金属硫化物呈细脉浸染状或浸染状分布, 该阶段是主要铜矿化阶段, 伴随硅化、绢云母化; 晚阶段发育石英、方解石和黄铁矿等(刘驰等, 1995; 武广等, 2009; 赵元艺等, 2011)。

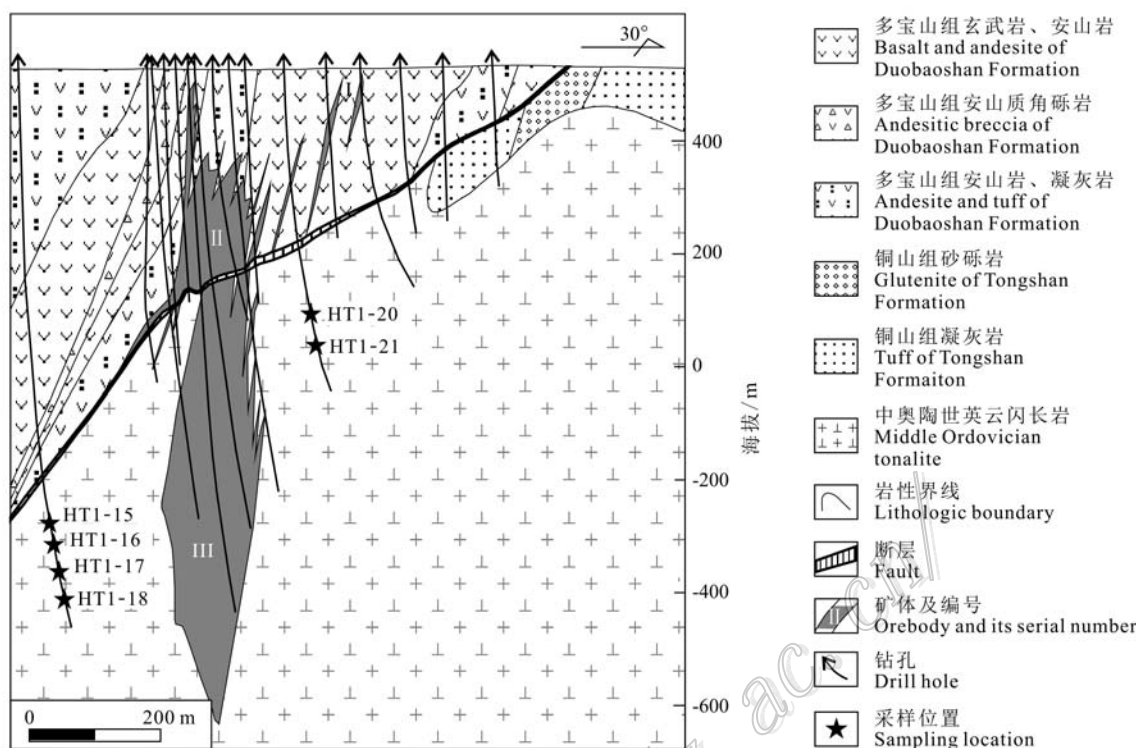


图3 铜山矿床1088线剖面图(据黑龙江省地质矿产局, 1993)

Fig. 3 Geological cross section along exploration line 1088 of the Tongshan deposit (after Heilongjiang Bureau of Geology and Mineral Resources, 1993)

3 样品特征及测试方法

3.1 样品特征

用于锆石U-Pb定年、岩石主微量元素及Hf同位素分析的英云闪长岩样品采自ZK737和ZK713钻孔, 采样位置见图3。采样时, 尽量采集无矿化且较新鲜的岩石, 但部分样品仍可见后期热液活动引起的青磐岩化现象。英云闪长岩样品呈花岗结构, 由斜长石(50% ~ 60%)、石英(20% ~ 30%)、角闪石(5% ~ 10%)及黑云母(5% ~ 10%)组成。斜长石多呈半自形板状, 聚片双晶发育, 部分绢云母化, 粒径0.5 ~ 3 mm。石英呈他形粒状充填在斜长石颗粒之间, 见波状消光, 粒径0.3 ~ 1.5 mm。角闪石呈长柱状, 局部被绿泥石、绿帘石交代, 粒径0.2 ~ 0.5 mm。黑云母大部分被绢云母和绿泥石交代, 粒径0.2 ~ 1.0 mm。副矿物见锆石、榍石和磁铁矿等。用于硫、铅同位素测试的黄铁矿单矿物样品选自I号矿体的石英-多金属硫化物脉。

3.2 测试方法

3.2.1 锆石U-Pb定年

将采集的英云闪长岩样品破碎, 按重力和磁选方法分选, 最后在双目镜下根据锆石颜色、自形程度、形态等特征初步分类, 挑选出具有代表性的锆石。将分选好的锆石用环氧树脂制靶、打磨和抛光。锆石的阴极发光(CL)图像在北京锆年领航科技有限公司完成, 仪器为日本JEOL公司生产的JSM 6510型扫描电子显微镜。LA-MC-ICP-MS锆石U-Pb定年测试工作在中国地质科学院矿产资源研究所国土资源部成矿作用与资源评价重点实验室完成, 锆石定年分析所用仪器为Finnigan Neptune型MC-ICP-MS及与之配套的Newwave UP 213激光剥蚀系统。激光剥蚀所用斑束直径为25 μm, 频率为10 Hz, 能量密度约为2.5 J/cm², 以He为载气。信号较小的²⁰⁷Pb、²⁰⁶Pb、²⁰⁴Pb(+²⁰⁴Hg)、²⁰²Hg用离子计数器(multi-ion-counters)接收, ²⁰⁸Pb、²³²Th、²³⁸U信号用法拉第杯接收, 实现了所有目标同位素信号的同时接收, 并且不同质量数的峰基本上都是平坦的, 进而

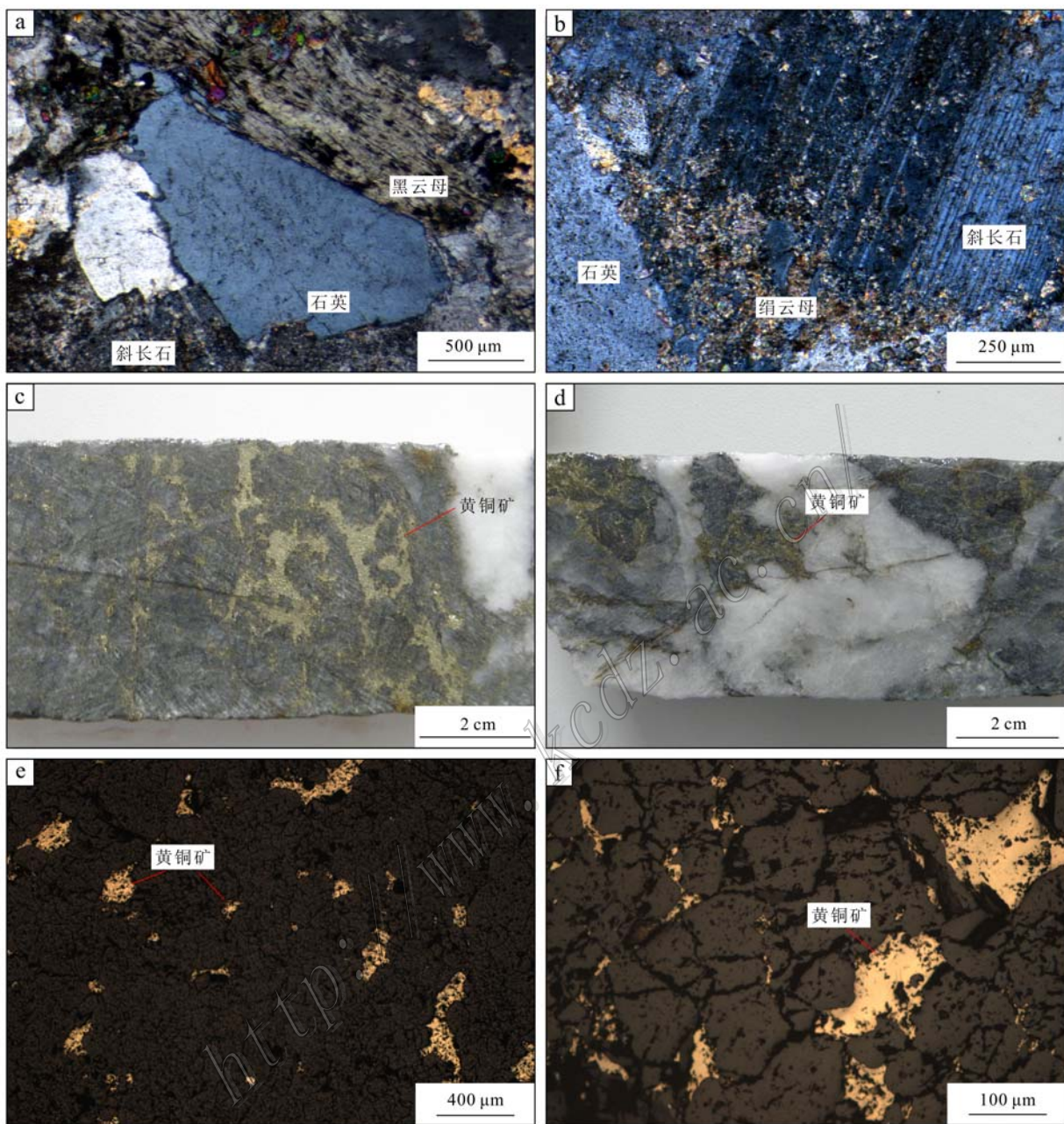


图4 铜山矿床典型岩/矿石手标本及显微照片

a. 英云闪长岩, 半自形粒状结构; b. 英云闪长岩, 半自形粒状结构; c. 黄铜矿, 浸染状结构; d. 石英-黄铜矿脉; e. 他形粒状黄铜矿; f. 半自形-他形粒状黄铜矿

Fig. 4 Hand specimens or microscope photographs of rock/ores from the Tongshan deposit

a. Tonalite, subhedral granular texture; b. Tonalite, subhedral granular texture; c. Chalcopyrite, disseminated texture;
d. Quartz-chalcopyrite vein; e. Anhedral granular chalcopyrite; f. Subhedral -anhedral granular chalcopyrite

可以获得高精度的数据, 均匀锆石颗粒 $^{207}\text{Pb}/^{206}\text{Pb}$ 、 $^{206}\text{Pb}/^{238}\text{U}$ 、 $^{207}\text{Pb}/^{235}\text{U}$ 的测试精度均为2%左右, 对锆石标准的定年精度和准确度在1%左右。测试过程中, 在每测定5~7个样品后, 重复测定两个锆石GJ1对样品进行校正, 并测量一个锆石Plesovice, 观

察仪器的状态以保证测试的精确度。详细实验测试过程见侯可军等(2009)。

3.2.2 岩石主量、微量元素分析

5件英云闪长岩样品的主量、微量元素测试工作在中国科学院地球化学研究所矿床地球化学国家重点

点实验室完成,其中主量元素采用 Axios PW4400型X射线荧光光谱仪(XRF)分析,分析误差小于5%,微量元素和稀土元素分析采用 Finnigan MAT公司的ELEMENT型ICP-MS分析,分析精度优于10%。

3.2.3 锆石Lu-Hf同位素分析

锆石完成U-Pb定年后,在原位用LA-MS-ICP-MS进行Lu-Hf同位素分析,测试工作在国土资源部成矿作用与资源评价重点实验室完成。实验过程中采用He作为剥蚀物质载气,剥蚀直径为55 μm,测定时使用锆石国际标样GJ1作为参考物质,分析点与U-Pb定年分析点相同。分析过程中锆石标准GJ1的¹⁷⁶Hf/¹⁷⁷Hf测试加权平均值为0.282 008±0.000 025(2σ, n=26)。相关仪器运行条件及详细分析流程见侯可军等(2007)。

3.2.4 硫、铅同位素分析

硫化物样品的硫、铅同位素分析在核工业北京地质研究院分析测试研究中心完成。硫同位素组成的测定方法:硫化物单矿物和氧化亚铜按一定比例研磨至200目左右,并混合均匀,在真空达2.0×10⁻²Pa状态下加热,进行氧化反应,反应温度为980℃,生成二氧化硫气体。在真空条件下,用冷冻法收集二氧化硫气体,并用MAT 253气体同位素质谱分析硫同位素组成。分析精度优于±0.2‰。硫化物参考标准为GBW-04414、GBW-04415硫化银标准,其δ³⁴S分别为-0.07‰±0.13‰和22.15‰±0.14‰。

铅同位素组成的测定方法:称取适量样品放入聚四氟乙烯坩埚中,加入氢氟酸、高氯酸溶解。样品分解后,将其蒸干,再加入盐酸溶解蒸干,加入0.5 mol/L的HBr溶液溶解样品进行铅的分离。将溶解的样品溶解倒入预先处理好的强碱性阴离子交换树脂中进行铅的分离,用0.5 mol/L的HBr溶液淋洗

树脂,再用2 mol/L的HCl溶液淋洗树脂,最后用6 mol/L的HCl溶液解脱,将解脱溶液蒸干备质谱测定。用热表面电离质谱法进行铅同位素测量,仪器型号为ISOPROBE-T,对1 μg的²⁰⁸Pb/²⁰⁶Pb测量精度≤0.005%。

4 测试结果

4.1 锆石U-Pb定年

英云闪长岩中锆石大多呈长柱状,少量为短柱状,粒径集中在80~120 μm,无色透明或黄褐色,具清晰的生长韵律环带(图5)。16颗锆石的Th/U比值介于0.54~0.85,大于0.1;w(Th)介于43.2×10⁻⁶~116.2×10⁻⁶,平均值为76.0×10⁻⁶;w(U)介于79.3×10⁻⁶~170.7×10⁻⁶,平均值为112.3×10⁻⁶(表1)。据此认为锆石为岩浆成因。其中4颗锆石(点HT1-15.4、HT1-15.5、HT1-15.6、HT1-15.16)的谐和年龄分别为(506±5) Ma、(483±2) Ma、(483±2) Ma、(482±6) Ma,属于捕获的继承锆石。其他12颗锆石给出了(461±1) Ma(n=12, MSWD=0.2)的加权平均年龄(图6),代表了锆石的结晶年龄。

4.2 岩石主量、微量元素及稀土元素

英云闪长岩的w(SiO₂)和w(Al₂O₃)分别为62.5%~64.53%、14.77%~17.7%。w(K₂O)、w(Na₂O)及全碱含量w(K₂O+Na₂O)分别为1.5%~3.76%、2.47%~4.18%及5.68%~6.34%。Na₂O/K₂O比值变化较大(介于0.69~2.79),可能与岩体遭受不同程度的钾长石化、绢云母化有关。w(MgO)、w(CaO)和w(FeO^T)分别为1.29%~2.18%、3.18%~4.62%及4.54%~5.69%。铝

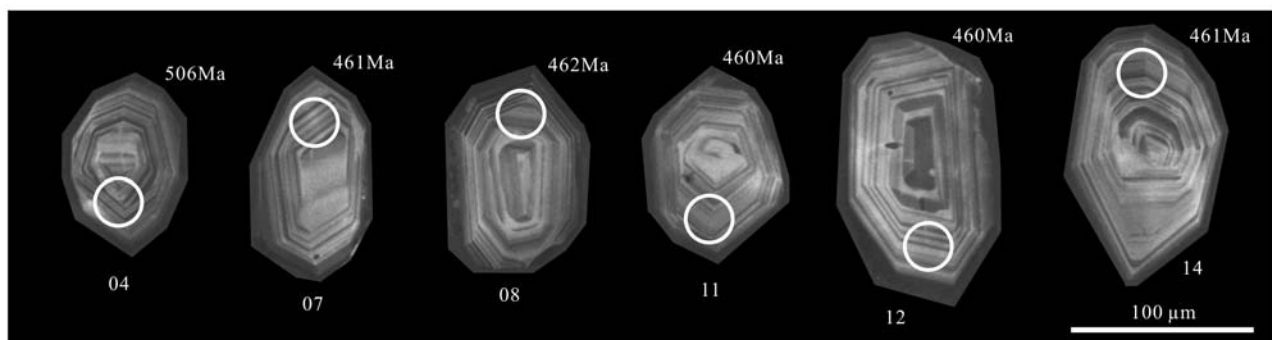


图5 铜山矿床英云闪长岩锆石代表性CL图像

Fig. 5 Representative cathodoluminescence (CL) images of zircons from the tonalite in the Tongshan deposit

表 1 铜山矿床 LA-MC-ICP-MS 锆石 U-Pb 分析结果
Table 1 LA-MC-ICP-MS zircon U-Pb data of the Tongshan deposit

样品号	$w_{\text{Pb}}/10^{-6}$		$^{207}\text{Pb}/^{206}\text{Pb}$	1σ	$^{207}\text{Pb}/^{235}\text{U}$	1σ	$^{206}\text{Pb}/^{238}\text{U}$	1σ	Th/U	$^{206}\text{Pb}/^{238}\text{U}$ 年龄/Ma	1σ	谐和性/%
	Th	U										
HT1-15.1	67.9	119.8	0.0592	0.0004	0.6035	0.0040	0.0740	0.0003	0.6	460	2	95
HT1-15.2	63.9	86.5	0.0562	0.0004	0.5731	0.0047	0.0740	0.0003	0.7	460	2	99
HT1-15.3	63.1	96.1	0.0581	0.0007	0.5938	0.0078	0.0741	0.0006	0.7	461	3	97
HT1-15.4	62.1	100.0	0.0598	0.0014	0.6736	0.0177	0.0817	0.0008	0.6	506	5	96
HT1-15.5	84.5	100.1	0.0603	0.0004	0.6472	0.0055	0.0778	0.0004	0.8	483	2	95
HT1-15.6	75.1	126.1	0.0592	0.0003	0.6355	0.0031	0.0779	0.0003	0.6	483	2	96
HT1-15.7	87.6	124.6	0.0579	0.0004	0.5911	0.0046	0.0741	0.0004	0.7	461	2	97
HT1-15.8	100.6	118.3	0.0598	0.0007	0.6134	0.0070	0.0743	0.0004	0.8	462	3	95
HT1-15.9	73.5	117.0	0.0590	0.0017	0.6032	0.0210	0.0741	0.0005	0.6	461	3	96
HT1-15.10	112.3	170.7	0.0597	0.0004	0.6125	0.0050	0.0744	0.0003	0.7	463	2	95
HT1-15.11	93.3	127.4	0.0585	0.0007	0.5959	0.0081	0.0739	0.0005	0.7	460	3	96
HT1-15.12	49.3	85.3	0.0565	0.0008	0.5771	0.0098	0.0740	0.0005	0.6	460	3	99
HT1-15.13	66.2	104.0	0.0595	0.0008	0.6061	0.0090	0.0739	0.0005	0.6	460	3	95
HT1-15.14	116.2	152.1	0.0570	0.0017	0.5821	0.0190	0.0741	0.0003	0.8	461	2	98
HT1-15.15	57.7	89.3	0.0594	0.0006	0.6092	0.0104	0.0743	0.0008	0.6	462	5	95
HT1-15.16	43.2	79.3	0.0595	0.0005	0.6367	0.0095	0.0776	0.0011	0.5	482	6	96

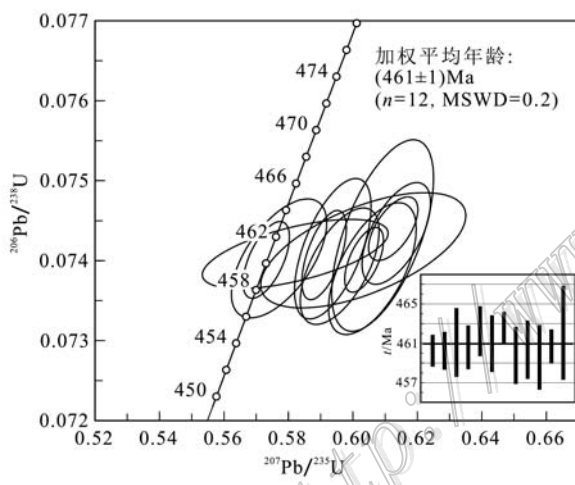


图 6 铜山矿床英云闪长岩锆石 U-Pb 谱和年龄图解

Fig. 6 Zircon U-Pb concordia diagram of the tonalite from the Tongshan deposit

指数 A/CNK 为 $1.00 \sim 1.23$ (表 2)。 ΣREE 介于 $51.63 \times 10^{-6} \sim 67.17 \times 10^{-6}$ 之间, $(\text{La}/\text{Yb})_N$ 为 $8.62 \sim 9.19$, 呈现轻稀土元素富集的右倾特征, δEu 值为 $0.96 \sim 1.09$, 主体显示较弱的铕正异常(图 7a)。同时富集 Ba、U、K、La、Sr、Sm 等元素, 亏损 Th、Ta、Nb、Ce、Nd、Ti 等元素(图 7b)。

4.3 锆石 Lu-Hf 同位素

12 颗锆石的 $^{176}\text{Yb}/^{177}\text{Hf}$ 和 $^{176}\text{Lu}/^{177}\text{Hf}$ 比值范围分别为 $0.017\ 128 \sim 0.034\ 905$ 、 $0.000\ 652 \sim 0.001\ 282$ 。 $^{176}\text{Lu}/^{177}\text{Hf}$ 比值小于 0.002, 表明这些锆石在形成后仅具有较少的放射成因 Hf 积累, 因此

可以用初始 $^{176}\text{Hf}/^{177}\text{Hf}$ 比值代表锆石形成时的 $^{176}\text{Hf}/^{177}\text{Hf}$ 比值(吴福元等, 2007)。锆石的 $\epsilon_{\text{Hf}}(t)$ 值为 $11.6 \sim 13.5$, 平均值为 12.7(图 8)。 $f_{\text{Lu/Hf}}$ 值介于 $-0.98 \sim -0.96$ 之间, 明显小于镁铁质地壳的 $f_{\text{Lu/Hf}}(-0.34$, Amelin et al., 2000) 和硅铝质地壳的 $f_{\text{Lu/Hf}}(-0.72$, Vervoort et al., 1996), 故二阶段模式年龄更能反映其源区物质从亏损地幔被抽取的时间(第五春荣等, 2007), 锆石 Hf 同位素二阶段模式年龄 t_{DM2} 为 $577 \sim 707$ Ma, 平均值为 635 Ma(表 3)。

4.4 硫、铅同位素

6 件黄铁矿样品的 $\delta^{34}\text{S}$ 值介于 $-1.3\text{‰} \sim -0.4\text{‰}$, 平均值为 -0.8‰ , 硫同位素分布区间狭小, 均值趋近零。铅同位素比值为 $^{206}\text{Pb}/^{204}\text{Pb} = 17.591 \sim 18.453$, $^{207}\text{Pb}/^{204}\text{Pb} = 15.449 \sim 15.551$, $^{208}\text{Pb}/^{204}\text{Pb} = 37.280 \sim 37.999$ (表 4)。

5 讨论

5.1 构造背景

古亚洲洋大约在 1000 Ma 前开始张开, 大规模扩张在 $700 \sim 600$ Ma, 在经历过若干微板块之间、微板块与南北大陆之间的碰撞之后, 直至二叠纪最终闭合(徐备等, 1997; Wu et al., 1998; 洪大卫等, 2003; 孙德有等, 2004; Li, 2006; 李锦铁等, 2007; Cao et al., 2013)。近年来, 对大兴安岭地区不同类型侵入岩和火山岩锆石 U-Pb 年代学的研究结果表明, 区

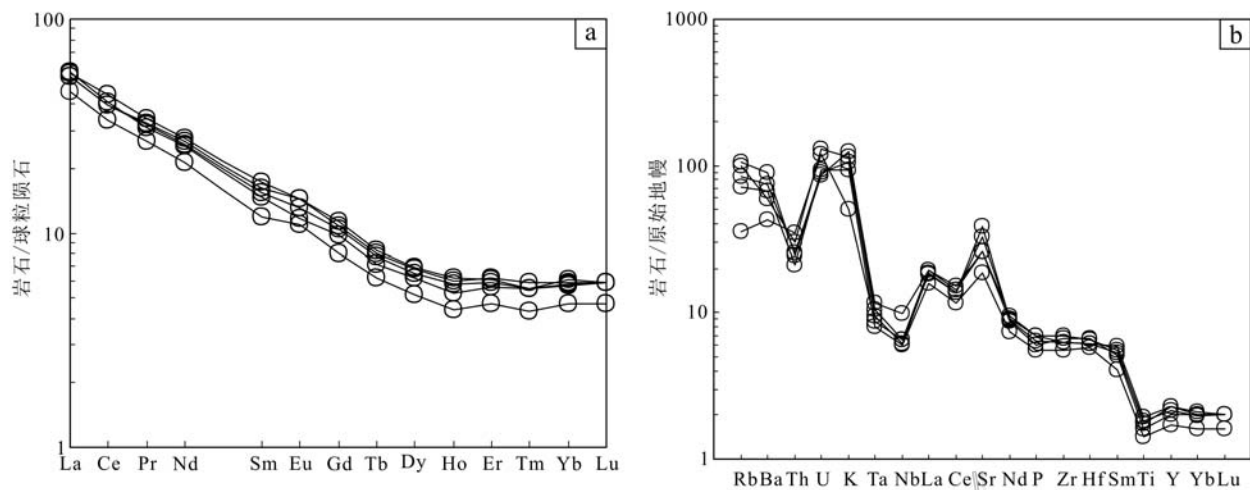


图 7 铜山矿床英云闪长岩稀土元素配分曲线和微量元素蛛网图(标准化数值分别采用 Boynton, 1984; Taylor et al., 1985)

Fig. 7 Chondrite-normalized REE patterns and primitive mantle normalized trace elements spider diagram of the tonalites from the Tongshan deposit (normalization values after Boynton, 1984; Taylor et al., 1985)

表 2 铜山矿床主量元素($w_B/\%$)、微量元素($w_B/10^{-6}$)及稀土元素($w_B/10^{-6}$)分析结果Table 2 Analyzed data of major elements ($w_B/\%$), trace and rare earth elements ($w_B/10^{-6}$) of the Tongshan deposit

组分	HT1-16	HT1-17	HT1-18	HT1-20	HT1-21	组分	HT1-16	HT1-17	HT1-18	HT1-20	HT1-21
SiO ₂	64.53	63.92	63.61	62.50	62.64	Ba	465	415	297	624	520
Al ₂ O ₃	14.77	15.15	17.68	17.36	17.70	La	10.9	13.4	12.7	13.3	12.8
FeO ^T	5.18	4.61	4.54	5.69	4.72	Ce	20.6	25.2	24.4	27.2	24.4
CaO	3.36	4.05	4.62	3.18	4.00	Pr	2.53	2.93	3.02	3.23	3.09
MgO	1.35	1.29	1.32	2.18	2.08	Nd	9.91	11.9	12.1	12.9	12.4
K ₂ O	2.84	3.47	1.5	3.76	3.21	Sm	1.82	2.26	2.37	2.62	2.46
Na ₂ O	2.99	2.47	4.18	2.58	2.93	Eu	0.63	0.68	0.76	0.83	0.83
MnO	0.06	0.07	0.08	0.09	0.10	Gd	1.64	2.01	2.13	2.33	2.21
TiO ₂	0.31	0.35	0.39	0.42	0.38	Tb	0.23	0.27	0.29	0.31	0.3
P ₂ O ₅	0.12	0.13	0.14	0.15	0.15	Dy	1.31	1.56	1.66	1.76	1.73
LOI	4.28	4.25	2.08	1.91	2.10	Ho	0.25	0.3	0.33	0.35	0.34
总和	99.79	99.76	100.14	99.82	100.01	Er	0.78	0.93	0.97	1.01	1.03
Na ₂ O/K ₂ O	1.05	0.71	2.79	0.69	0.91	Tm	0.11	0.14	0.14	0.14	0.15
K ₂ O+Na ₂ O	5.83	5.94	5.68	6.34	6.14	Yb	0.8	0.99	0.97	1.04	1
A/CNK	1.05	1.00	1.05	1.23	1.14	Lu	0.12	0.15	0.15	0.15	0.15
Mg [#]	34	36	37	43	47	Hf	1.77	2.07	1.89	1.91	2.03
Li	3.93	5.92	4.33	7.39	4.83	Ta	0.33	0.48	0.36	0.43	0.39
Be	0.91	1.27	1.03	1.07	1.05	W	3.28	4.79	7.9	5.95	3.8
Sc	8.4	8.79	11.2	10.5	10.7	Tl	0.15	0.2	0.09	0.23	0.2
V	93.7	90	112	112	105	Pb	8.02	21.4	9.54	7.85	8.88
Cr	16.3	21.3	20.6	16.3	23.2	Bi	0.719	0.701	0.369	0.652	0.387
Co	23.9	8.78	7.54	13.6	9.15	Th	1.81	2.55	2.96	2.07	2.16
Ni	8.39	8.58	10.10	8.55	12.4	U	1.98	2.72	2.52	1.8	1.87
Ga	14.6	15.4	17.0	18.0	17.0	Cd	0.191	0.342	0.181	0.277	0.176
Ge	1.13	1.25	1.33	1.24	1.16	Σ REE	51.63	62.72	61.99	67.17	62.89
As	3.23	2.07	1.92	1.64	1.88	δ Eu	1.09	0.96	1.01	1.01	1.07
Rb	45.3	63.0	22.5	66.8	53.7	La/Yb	13.63	13.54	13.09	12.79	12.8
Sr	394	543	804	546	682	(La/Yb) _N	9.19	9.13	8.83	8.62	8.63
Y	7.78	9.08	9.81	10.30	10.30	Sr/Y	50.64	59.8	81.96	53.01	66.21
Zr	62.5	75	69.8	70.4	77.8	La/Nb	2.53	1.92	2.71	2.87	2.91
Nb	4.30	6.99	4.69	4.63	4.40	Ba/Nb	108.14	59.37	63.33	134.77	118.18
In	0.054	0.065	0.038	0.076	0.036	Ba/La	42.66	30.97	23.39	46.92	40.63
Sn	1.75	2.26	2.39	1.80	2.00	Ba/Th	256.91	162.75	100.34	301.45	240.74
Sb	1.14	1.53	1.14	0.33	0.41	Zr/Nb	14.53	10.73	14.88	15.21	17.68
Cs	1.32	2.32	0.46	1.40	1.05	Th/Yb	2.26	2.58	3.05	1.99	2.16

注: 比值单位为 1。

表 3 铜山矿床英云闪长岩锆石 Hf 同位素数据

Table 3 Zircon Hf isotopic compositions of the tonalite from the Tongshan deposit

测点号	年龄/Ma	$^{176}\text{Yb}/^{177}\text{Hf}$	2σ	$^{176}\text{Lu}/^{177}\text{Hf}$	2σ	$^{176}\text{Hf}/^{177}\text{Hf}$	2σ	$(^{176}\text{Hf}/^{177}\text{Hf})_t$	$\epsilon_{\text{Hf}}(t)$	t_{DM}/Ma	t_{DM2}/Ma	$f_{\text{Lu/Hf}}$
HT1-15.1	460	0.027015	0.000226	0.001026	0.000005	0.282846	0.000011	0.282837	2.6	12.5	576	645
HT1-15.2	460	0.027043	0.000855	0.001072	0.000030	0.282872	0.000016	0.282862	3.5	13.4	540	588
HT1-15.3	461	0.025905	0.000506	0.000990	0.000016	0.282825	0.000017	0.282816	1.9	11.8	605	691
HT1-15.4	506	0.034976	0.000669	0.001306	0.000026	0.282796	0.000017	0.282783	0.8	11.6	652	737
HT1-15.5	483	0.027393	0.000421	0.001076	0.000017	0.282859	0.000015	0.282849	3.1	13.4	557	602
HT1-15.6	483	0.030413	0.000235	0.001154	0.000008	0.282820	0.000014	0.282810	1.7	12.0	614	692
HT1-15.7	461	0.034905	0.001034	0.001282	0.000034	0.282830	0.000016	0.282819	2.1	11.9	602	684
HT1-15.8	462	0.028489	0.000282	0.001084	0.000008	0.282839	0.000013	0.282830	2.4	12.3	586	660
HT1-15.9	461	0.030725	0.000454	0.001177	0.000013	0.282862	0.000016	0.282852	3.2	13.0	555	611
HT1-15.10	463	0.029045	0.000192	0.001102	0.000010	0.282818	0.000015	0.282809	1.6	11.6	616	707
HT1-15.11	460	0.021952	0.000938	0.000849	0.000039	0.282874	0.000014	0.282866	3.6	13.5	534	579
HT1-15.12	460	0.029526	0.001030	0.001119	0.000039	0.282877	0.000015	0.282867	3.7	13.5	533	577
HT1-15.13	460	0.017128	0.000156	0.000652	0.000004	0.282862	0.000014	0.282856	3.2	13.2	548	602
HT1-15.14	461	0.025410	0.000204	0.000955	0.000008	0.282842	0.000013	0.282834	2.5	12.4	579	651
HT1-15.15	462	0.019972	0.000400	0.000753	0.000012	0.282849	0.000012	0.282843	2.7	12.7	566	630
HT1-15.16	482	0.025669	0.000221	0.000958	0.000011	0.282841	0.000013	0.282832	2.4	12.8	582	642

注: $\epsilon_{\text{Hf}}(0) = 10000 \times [(\frac{(^{176}\text{Hf}/^{177}\text{Hf})_s - (^{176}\text{Hf}/^{177}\text{Hf})_{\text{CHUR},0}}{(^{176}\text{Hf}/^{177}\text{Hf})_s} \times (e^{\lambda t} - 1)] \times [(\frac{(^{176}\text{Lu}/^{177}\text{Hf})_s - (^{176}\text{Lu}/^{177}\text{Hf})_{\text{CHUR},0}}{(^{176}\text{Lu}/^{177}\text{Hf})_s} \times (e^{\lambda t} - 1)] - 1]$. $t_{\text{DM}} = 1/\lambda$
 $\times \ln \frac{(^{176}\text{Hf}/^{177}\text{Hf})_s - (^{176}\text{Hf}/^{177}\text{Hf})_{\text{DM}}}{(^{176}\text{Hf}/^{177}\text{Hf})_s - (^{176}\text{Lu}/^{177}\text{Hf})_{\text{DM}}}$. $t_{\text{DM2}} = t_{\text{DM}} - t(t_{\text{DM}} - t)$. $t_{\text{DM2}} = t_{\text{DM}} - t(f_{\infty} - f_s)$. $f_{\text{Lu/Hf}} = (^{176}\text{Lu}/^{177}\text{Hf})_{\text{CHUR}} - 1$. $(^{176}\text{Hf}/^{177}\text{Hf})_{\text{t}} = (^{176}\text{Hf}/^{177}\text{Hf})_s - (^{176}\text{Hf}/^{177}\text{Hf})_s \times (^{176}\text{Lu}/^{177}\text{Hf})_s$. 其中 $\lambda = 1.867 \times 10^{-11}/a$ (Soderlund et al., 2004); $(^{176}\text{Lu}/^{177}\text{Hf})_s$ 和 $(^{176}\text{Hf}/^{177}\text{Hf})_s$ 为样品测量值; $(^{176}\text{Lu}/^{177}\text{Hf})_{\text{CHUR}} = 0.0332$, $(^{176}\text{Hf}/^{177}\text{Hf})_{\text{CHUR},0} = 0.282772$; $(^{176}\text{Lu}/^{177}\text{Hf})_{\text{DM}} = 0.0384$, $(^{176}\text{Hf}/^{177}\text{Hf})_{\text{DM}} = 0.28325$ (Blichert-Toft et al., 1997; Griffin et al., 2000); $(^{176}\text{Lu}/^{177}\text{Hf})_{\text{平均地壳}} = 0.015$; $f_{\infty} = [(^{176}\text{Lu}/^{177}\text{Hf})_{\text{平均地壳}} / (^{176}\text{Lu}/^{177}\text{Hf})_{\text{CHUR}}] - 1$; t 为锆石结晶年龄。

表 4 铜山矿床硫、铅同位素组成

Table 4 Sulfur and lead isotopic compositions of the Tongshan deposit

样号	金属矿物	$\delta^{34}\text{S}/\text{‰}$	$^{208}\text{Pb}/^{204}\text{Pb}$	2σ	$^{207}\text{Pb}/^{204}\text{Pb}$	2σ	$^{206}\text{Pb}/^{204}\text{Pb}$	2σ	μ
HT-3	黄铁矿	-0.4	37.999	0.005	15.551	0.002	18.067	0.003	9.41
HT-9	黄铁矿	-0.6	37.682	0.008	15.513	0.003	18.340	0.004	9.30
HT-10	黄铁矿	-0.8	37.638	0.01	15.525	0.004	18.453	0.005	9.31
HT-18	黄铁矿	-1.1	37.866	0.003	15.521	0.001	17.951	0.002	9.36
HT-19	黄铁矿	-1.3	37.280	0.005	15.449	0.002	17.591	0.002	9.27
HT-19-1	黄铁矿	-0.7	37.500	0.008	15.485	0.003	17.691	0.004	9.32

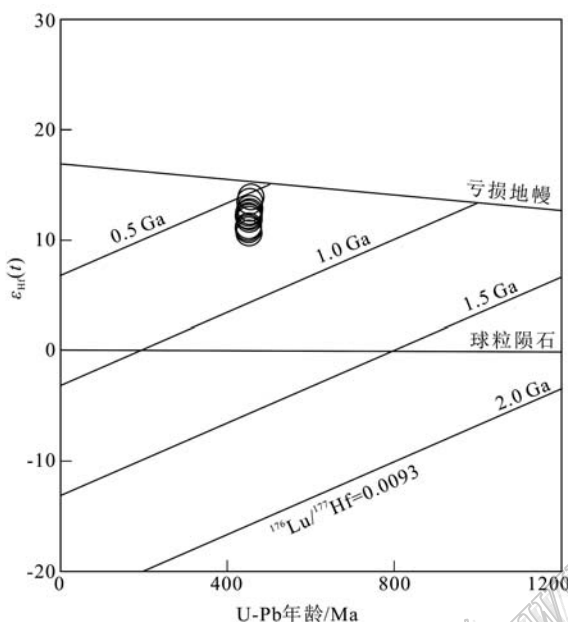
图 8 铜山矿床英云闪长岩锆石 $\epsilon_{\text{Hf}}(t)$ 与 U-Pb 年龄图解

Fig. 8 Plot of $\epsilon_{\text{Hf}}(t)$ versus U-Pb ages for the tonalite from the Tongshan deposit

域上存在大规模的早古生代岩浆-热液活动(Guo et al., 2009)。大兴安岭南部出露具有埃达克岩地球化学特征的石英闪长岩、奥长花岗岩、斜长岩及英安岩(SHRIMP 锆石 U-Pb 年龄为 428 ~ 467 Ma, 刘敦一等, 2003)和闪长-花岗岩类(SHRIMP 锆石 U-Pb 年龄为 464 ~ 490 Ma, 石玉若等, 2004), 该区存在早古生代古亚洲洋板片的俯冲作用(Jian et al., 2008)。Ge 等(2005; 2007)在大兴安岭北部发现了早古生代辉长岩(LA-ICP-MS 锆石 U-Pb 年龄为 480 ~ 494 Ma)和花岗闪长岩(SHRIMP 锆石 U-Pb 年龄为 (485 ± 8) Ma), 认为古生代区域上发生了从俯冲消减到碰撞后阶段的演化过程, 而施光海等(2003)、Pei 等(2007)和 Miao 等(2007)在一些深变质杂岩中也发现了早古生代岩浆锆石。余宏全等(2012)对大兴安岭中北段岩浆岩的锆石 U-Pb 年龄进行了统计,

认为该地区在古生代期间经历了古陆块间的俯冲、拉张、拼贴碰撞的构造演化历史。综上所述, 晚寒武世—早志留世期间, 古亚洲洋在大兴安岭地区存在强烈的与俯冲作用有关的岩浆活动。

铜山矿床英云闪长岩体位于大兴安岭北部, 形成于中奥陶世, 岩石富集大离子亲石元素(如 Rb、Ba 和 Sr), 稀土元素呈现右倾斜式模型, 相对亏损高场强元素(如 Ti、Nb 和 Ta), 显示出较高的 La/Nb ($1.92 \sim 2.91$)、Ba/Nb($59.37 \sim 134.77$)、Ba/La ($23.39 \sim 46.92$)、Ba/Th($100.34 \sim 301.45$)、Zr/Nb($10.73 \sim 17.68$)比值和低的 Th/Yb 比值($1.99 \sim 3.05$)、低的 $w(\text{TiO}_2)$ ($< 1\%$), 具有俯冲环境下岩浆岩的地球化学特征(Kelemen et al., 1990; Hawkesworth et al., 1991; Woodhead et al., 1993; Pearce et al., 1999; Stern, 2002; Zhou et al., 2004), Ti、Nb、Ta 的负异常及 HREE 亏损暗示着岩浆源区有钛铁矿、金红石、榍石、石榴子石等矿物的残留(Green et al., 1986)。在 Yb-Ta 图解(图 9a)中, 英云闪长岩样品落入火山弧花岗岩区域, 在 Y-Nb 图解(图 9b)中, 样品落入火山弧和同碰撞花岗岩区域, 在 R1-R2 图解(图 9c)中, 样品落入板块碰撞前区域, 在 Nb/Yb-Th/Yb 图解(图 9d)中, 样品落入大陆弧区域。综合区域构造-岩浆演化资料, 作者认为铜山矿床英云闪长岩形成于大陆边缘弧环境。

5.2 岩石属性及源区

埃达克岩是 Defant 等(1990)研究阿留申群岛新生代俯冲洋壳熔融产生的火山岩时提出来的术语, 用于概括具有特定地球化学性质的一套中酸性火山岩和侵入岩组合, 包括安山岩、英安岩、安粗岩、石英闪长岩、花岗闪长岩、石英二长岩、英云闪长岩和斜长花岗岩等, 其地球化学标志是 $w(\text{SiO}_2) \geqslant 56\%$, $w(\text{Al}_2\text{O}_3) \geqslant 15\%$, $w(\text{MgO}) < 3\%$, $\text{Na}_2\text{O}/\text{K}_2\text{O} > 2.4$, Y 和重稀土元素(HREE)含量低($w(\text{Yb}) \leqslant 1.9 \times 10^{-6}$ 、 $w(\text{Y}) \leqslant 18 \times 10^{-6}$), 高 Sr(大多数 $> 400 \times$

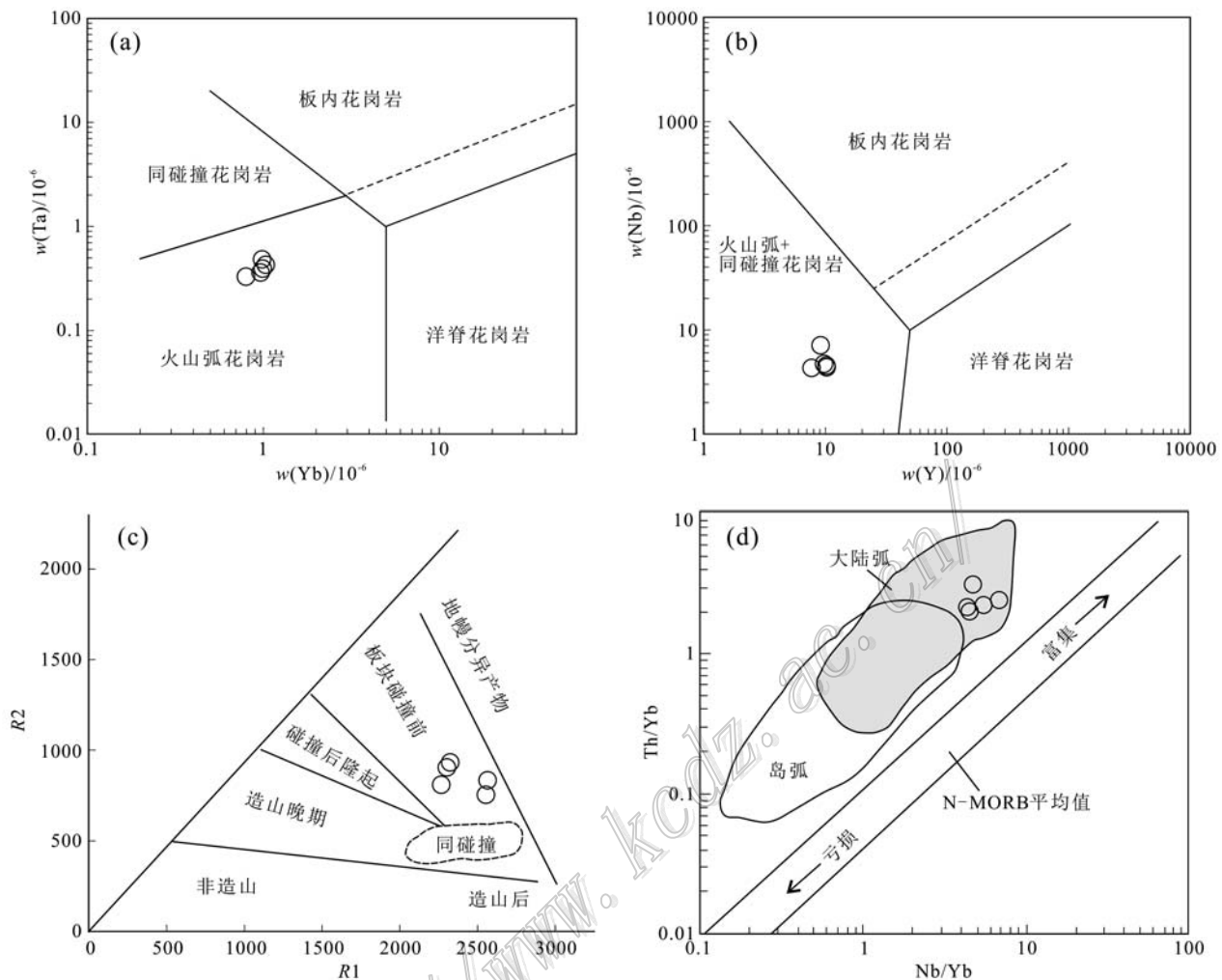


图9 铜山矿床构造环境判别图解

(a). Yb-Ta关系图(底图据 Pearce et al., 1984);(b). Y-Nb关系图(底图据 Pearce et al., 1984);(c). R1与R2判别图
(底图来自 De La Roche et al., 1980);(d). Nb/Yb-Th/Yb关系图(底图据 Pearce et al., 1995)

Fig. 9 Tectonic discrimination diagrams of the Tongshan deposit

(a). Yb-Ta diagram (after Pearce et al., 1984); (b). Y-Nb diagram (after Pearce et al., 1984); (c). R1-R2 diagram (after De La Roche et al., 1980); (d). Nb/Yb-Th/Yb diagram (after Pearce et al., 1995)

10^{-6}),一般具有正铕异常(少数具有极弱负铕异常)。然而,具有上述地球化学特征、与俯冲洋壳熔融无关的岩石通常被称为“埃达克质(adakitic)岩”(Castillo, 2006; 2012)。铜山矿床英云闪长岩显示了与埃达克岩相似的地球化学特征,其 $w(\text{SiO}_2)$ 为 $62.50\% \sim 64.53\%$, $w(\text{Al}_2\text{O}_3)$ 为 $14.77\% \sim 17.70\%$, $w(\text{MgO})$ 为 $1.29\% \sim 2.18\%$, $w(\text{Sr})$ 为 $394 \times 10^{-6} \sim 804 \times 10^{-6}$, $w(\text{Y})$ 为 $7.78 \times 10^{-6} \sim 10.3 \times 10^{-6}$, $w(\text{Yb})$ 为 $0.8 \times 10^{-6} \sim 1.04 \times 10^{-6}$,轻稀土元素富集,重稀土元素亏损,显示较弱的Eu异常($\delta\text{Eu} = 0.96 \sim 1.09$)。在 Sr/Y-Y 图解(图

10a)和 $(\text{La}/\text{Yb})_{\text{N}}-\text{Yb}_{\text{N}}$ 图解(图 10b)中,英云闪长岩样品均位于埃达克岩区域。

在 SiO_2-MgO 图解(图 11)中,铜山矿床英云闪长岩样品落入增厚下地壳熔融形成的埃达克质岩区,部分样品临近俯冲洋壳熔融形成的埃达克岩区。大量研究(Smithies, 2000; Defant et al., 2001; 2002; Xu et al., 2002)表明,俯冲洋壳熔融形成的埃达克岩、拆沉下地壳熔融形成的埃达克质岩均具有较高的MgO含量,是由于俯冲洋壳和拆沉下地壳熔融产生的熔体穿过地幔的过程中,熔体与地幔橄榄岩发生了反应,导致熔体的MgO和相容元素(Cr、

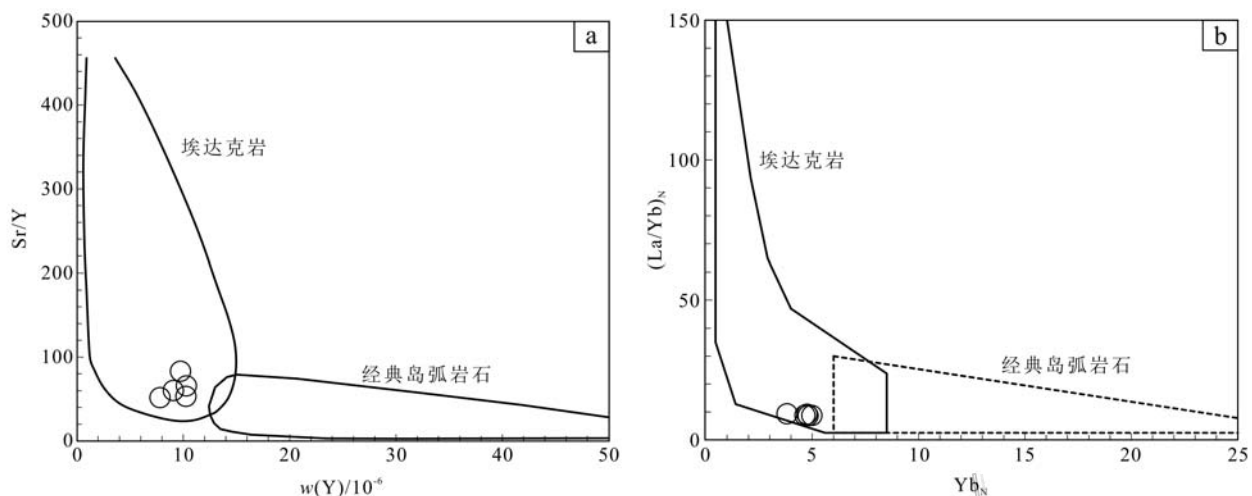
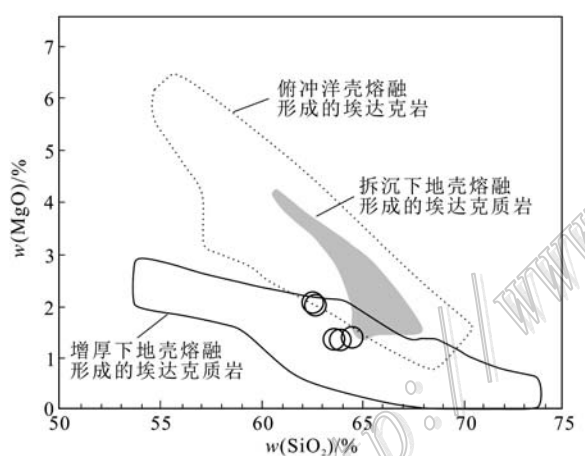
图 10 铜山矿床英云闪长岩 Sr/Y-Y(a, 底图据 Defant et al., 1990) 和 (La/Yb)_N-Yb_N 关系图解(b, 底图据 Martin, 1999)

Fig. 10 Sr/Y-Y (a, after Defant et al., 1990) and (La/Yb)_N-Yb_N (b, after Martin, 1999) diagrams discriminating between adakitic and classical arc calc-alkaline compositions for tonalites from the Tongshan deposit

图 11 铜山矿床英云闪长岩 MgO-SiO₂ 判别图

俯冲洋壳熔融的埃达克质岩引自文献 Defant et al., 1990; 2002; Martin, 1999; 拆沉下地壳熔融形成的埃达克质岩引自文献 Xu et al., 2002; 增厚下地壳熔融形成的埃达克质岩引自文献 Atherton et al., 1993; Muir et al., 1995; Johnson et al., 1997; Xiong et al., 2003; Wang et al., 2006

Fig. 11 MgO-SiO₂ diagram for the tonalites from the Tongshan deposit

Fields of subducted oceanic crust-derived adakites after Defant et al., 1990; 2002; Martin, 1999; Delaminated lower crust-derived adakitic rocks after Xu et al., 2002; Field of thick lower crust-derived adakitic rocks after Atherton et al., 1993; Muir et al., 1995; Johnson et al., 1997; Xiong et al., 2003; Wang et al., 2006

Ni)含量增高。铜山矿床英云闪长岩与增厚下地壳熔融形成的埃达克质岩具有较一致的 MgO 含量, 较

低的 Mg[#] (34 ~ 47, 均值为 39) 和相容元素含量 ($w(\text{Cr}) = 16.3 \times 10^{-6} \sim 23.2 \times 10^{-6}$, $w(\text{Ni}) = 8.39 \times 10^{-6} \sim 12.4 \times 10^{-6}$), 表明这些具埃达克岩地球化学特征的英云闪长岩来自于增厚下地壳的部分熔融。一般认为, 由地幔熔融产生高 SiO₂ 含量的花岗质岩浆是十分困难和有限的, 具有正 $\epsilon_{\text{Hf}}(t)$ 值的花岗质岩石一般来自亏损地幔或亏损地幔中新增生的年轻地壳物质的部分熔融(孙德有等, 2005; 隋振民等, 2007)。铜山矿床英云闪长岩的 Hf 同位素组成, 揭示其源区是新元古代期间从亏损地幔新增生的年轻下地壳。一种可能的成岩机制是: 中奥陶世, 古亚洲洋板块以缓倾角向西伯利亚大陆俯冲, 这种缓俯冲消减过程会引起大规模地壳缩短加厚, 使得脱水消减板片上的楔状地幔变冷而缺乏流动性, 限制了地幔楔的部分熔融规模和流体溢出(Kay et al., 2001)。从这种地幔产生的基性熔体底侵于加厚下地壳底部, 必然使下地壳越来越富水并发生部分熔融作用, 最终形成埃达克质英云闪长岩。这种在加厚陆壳条件下新生的水化基性下地壳的部分熔融机制, 与秘鲁北部高安第斯地区 Cordillera Blanca 岩基的花岗质岩石成因相似(Atherton et al., 1993; Petford et al., 1992; 1996a; 1996b; 2001; 刘红涛等, 2004)。

5.3 成矿意义

埃达克岩或埃达克质岩与斑岩型和浅成低温热

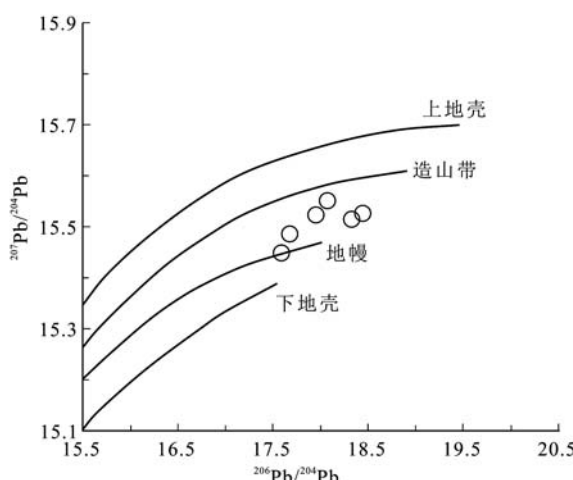


图 12 铜山矿床 $^{207}\text{Pb}/^{204}\text{Pb}$ - $^{206}\text{Pb}/^{204}\text{Pb}$ 图解
(底图据 Zartman et al., 1981)

Fig. 12 Diagram of lead isotopic compositions of the Tongshan deposit (after Zartman et al., 1981)

液型金-铜的成矿系统关系密切(Thiéblemont et al., 1997; Sajona et al., 1998; Bellon et al., 2001; Oyarzun et al., 2001; Defant et al., 2002; Mungall, 2002; 侯增谦等, 2005; 莮宗瑶等, 2006; 刘云飞等, 2012; 曲晓明等, 2012; 曹康等, 2014)。Thiéblemont 等(1997)统计了全球 43 个 Au、Ag、Cu、Mo 低温热液矿床和斑岩矿床,发现其中的 38 个与埃达克岩有关,显示出埃达克岩对 Cu-Au-Mo 矿化作用具有明显的倾向性。Sajona 等(1998)研究了菲律宾的斑岩铜矿和浅成低温热液矿床,发现 14 个矿床中有 12 个与埃达克岩有关。近年来,中国学者也陆续报道了很多与 Cu-Au-Mo-Ag-Fe 矿化密切共生的埃达克质岩(张旗等, 2004; 王强等, 2003; 2008; 谢建成等, 2012; 王金荣等, 2013; 陈希节等, 2014)。埃达克岩有利成矿的关键因素与埃达克岩形成时角闪石转变为石榴子石的脱水作用有关(Kay et al., 2001)。埃达克质岩浆的富流体、高氧逸度和基性源岩等固有属性,有利于铜、金等深源金属元素的萃取和富集成矿(武广等, 2008)。铜山矿床英云闪长岩属于埃达克质岩石,演化于加厚下地壳的部分熔融。铜山矿床金属硫化物的 $\delta^{34}\text{S}$ 值介于 $-1.3\text{\textperthousand} \sim -0.4\text{\textperthousand}$ (平均值 $-0.8\text{\textperthousand}$),表明硫主要来源于深源岩浆。铜山矿床矿石铅同位素投影点基本落在地幔演化线附近(图 12),其 μ 值为 $9.27 \sim 9.41$ (平均值 9.33),接近地幔的 μ 值(9.30 , Hart, 1988),反映了幔源铅的特征,这与英云闪长岩的下地壳岩浆源区特征相符合,

揭示成岩成矿物质可能来自于亏损地幔增生的下地壳。最近研究(杜琦等, 1988; 赵元艺等, 2011)揭示,铜山矿床所处的北西向弧形构造带外侧存在一个面积达 228 km^2 的 Cu 元素降低场,赋矿地层多宝山组火山岩的平均 $w(\text{Cu})$ 达 130×10^{-6} ,而多宝山矿田弱青磐岩化带内多宝山组火山岩的平均 $w(\text{Cu})$ 降低为 58×10^{-6} ,暗示多宝山组火山岩可能为区域上另一个重要的矿源层。

中奥陶世,古亚洲洋板片以缓倾角向西伯利亚大陆俯冲,陆壳加厚时水化基性下地壳的部分熔融形成富 Cu、Mo 等元素的中酸性埃达克质岩浆,其上升侵位到多宝山组火山岩中,岩浆流体驱动外围的大气降水对流循环,被加热的地下水和围岩发生水岩交换反应,进一步萃取了围岩中 Cu、Mo 等金属元素,当成矿流体运移至浅部时,由于构造减压作用,发生成矿流体的不混溶或沸腾作用(武广等, 2009),造成大规模铜等成矿元素沉淀下来,形成铜山铜矿床。在加厚陆壳条件下新生的水化基性下地壳的部分熔融生成的岩浆富含成矿所需要的大量挥发分和水流体,有利于岩浆中成矿物质(Cu、Au、Mo 等)的循环和萃取(刘红涛等, 2004)。这种岩浆-成矿作用类似于智利中部中安第斯缓消减带之上发生的岩浆活动及相伴的大规模 Cu-Au 成矿作用,在该地区已发现了 El Teniente(Rabbia et al., 2000)、Los Pelambres(Reich et al., 2003)、Rio Blanco-Los Brones(Kay et al., 1999)、El Indio-Pascua(Bissig et al., 2003)等世界级巨型和超大型斑岩铜矿床和浅成热液金矿床,而这些著名的斑岩铜矿床和浅成热液金矿床都与埃达克岩浆有关(Kay et al., 1999; 2001; 2002; Bissig et al., 2003; Reich et al., 2003; 刘红涛等, 2004)。成矿期后的铜山断裂既切断了矿体与矿化蚀变带,同时又起到了保护下盘矿体免遭剥蚀的重要作用(王喜臣等, 2007)。

6 结 论

(1) 铜山矿床英云闪长岩的 LA-MC-ICP-MS 锆石 U-Pb 年龄为 $(461 \pm 1)\text{ Ma}$, 形成于中奥陶世。岩石具有高 $w(\text{SiO}_2)$ ($62.5\% \sim 64.53\%$)、 $w(\text{Al}_2\text{O}_3)$ ($14.77\% \sim 17.7\%$) 和 $w(\text{Sr})$ ($394 \times 10^{-6} \sim 804 \times 10^{-6}$), 低 $w(\text{Y})$ ($7.78 \times 10^{-6} \sim 10.3 \times 10^{-6}$) 和 $w(\text{Yb})$ ($0.8 \times 10^{-6} \sim 1.04 \times 10^{-6}$), 轻稀土元素富集,重稀土元素亏损,无明显 Eu 异常等特征,显示出

埃达克质岩的地球化学特征。英云闪长岩形成于大陆边缘弧环境, 来源于加厚下地壳物质的部分熔融。

(2) 铜山矿床金属硫化物的 $\delta^{34}\text{S}$ 值介于 $-1.3\text{\textperthousand} \sim -0.4\text{\textperthousand}$, 平均值为 $-0.82\text{\textperthousand}$ 。铅同位素比值为 $^{206}\text{Pb}/^{204}\text{Pb} = 17.591 \sim 18.453$, $^{207}\text{Pb}/^{204}\text{Pb} = 15.449 \sim 15.551$, $^{208}\text{Pb}/^{204}\text{Pb} = 37.280 \sim 37.999$ 。成矿物质主要来自于英云闪长岩及多宝山组火山岩。

志 谢 野外工作期间得到了黑龙矿业集团股份有限公司梁海军经理、齐永生工程师等的大力支持。实验过程中得到了中国地质科学院矿产资源研究所侯可军博士、郭春丽副研究员的热情帮助。在此一并志以诚挚的感谢。

References

- Amelin Y, Lee D C and Halliday A N. 2000. Early-middle Archaean crustal evolution deduced from Lu-Hf isotopic studies of single zircon grains[J]. *Geochimica et Cosmochimica Acta*, 64: 4205-4225.
- Atherton M P and Petford N. 1993. Generation of sodium rich magmas from newly underplated basaltic crust[J]. *Nature*, 362: 144-146.
- Bellon H and Yumul Jr G P. 2001. Miocene to Quaternary adakites and related rocks in western Philippine arc sequences[J]. *Earth and Planetary Sciences*, 333: 343-350.
- Bissig T, Clark A H, Lee J K W and Quadt A. 2003. Petrogenetic and metallogenetic responses to Miocene slab flattening: New constraints from the E1 Indio-Pascua Au-Ag-Cu belt, Chile/Argentina [J]. *Mineralium Deposita*, 38: 84-862.
- Blichert-Toft J and Albarède F. 1997. The Lu-Hf geochemistry of chondrites and the evolution of the mantle-crust system[J]. *Earth and Planetary Science Letters*, 148: 243-258.
- Boynton W V. 1984. Cosmochemistry of the rare earth elements: Meteorite studies[J]. *Geochemistry*, 2: 63-114.
- Cao H H, Xu W L, Pei F P, Wang Z W, Wang F, Wang Z J. 2013. Zircon U-Pb geochronology and petrogenesis of the Late Paleozoic-Early Mesozoic intrusive rocks in the eastern segment of the northern margin of the North China Block[J]. *Lithos*, 170-171: 91-207.
- Cao K, Xu J F, Chen J L, Huang X X and Ren J B. 2014. Origin of porphyry intrusions hosting superlarge Pulang porphyry copper deposit in Yunnan Province: Implications for metallogenesis [J]. *Mineral Deposits*, 33(2): 307-322 (in Chinese with English abstract).
- Castillo P R. 2006. An overview of adakite petrogenesis[J]. *Chinese Science Bulletin*, 51: 257-268.
- Castillo P R. 2012. Adakite petrogenesis[J]. *Lithos*, 134: 304-316.
- Chen X J, Xu Z Q, Meng Y K and He Z Y. 2014. Petrogenesis of Miocene adakitic diorite-porphyrite in middle Gangdese batholith, southern Tibet: Constraints from geochemistry, geochronology and Sr-Nd-Hf isotopes[J]. *Acta Petrologica Sinica*, 30(8): 2253-2268 (in Chinese with English abstract).
- De La Roche H, Letterier J, Grandclaude P and Marchal M. 1980. A classification of volcanic and plutonic rocks using R1-R2 diagrams and major element analyses-its relationship with current nomenclature[J]. *Chemical Geology*, 29(1-4): 183-210.
- Defant M J and Drummond M S. 1990. Derivation of some modern arc magmas by melting of young subducted lithosphere [J]. *Nature*, 347(18): 662-665.
- Defant M J and Kepezhinskas P. 2001. Evidence suggests slab melting in arc magmas[J]. *EOS*, 82: 62-69.
- Defant M J, Xu J F, Kepezhinskas P, Wang Q, Zhang Q and Xiao L. 2002. Adakites: Some variations on a theme[J]. *Acta Petrologica Sinica*, 18: 129-142.
- Diwu C R, Sun Y, Lin C L, Liu X M and Wang H L. 2007. Zircon U-Pb ages and Hf isotopes and their geological significance of Yiyang TTG gneisses from Henan Province, China[J]. *Acta Petrologica Sinica*, 23(2): 253-262 (in Chinese with English abstract).
- Du Q, Zhao Y M, Lu B G, Ma D Y, Li P L, Lv J K, Li W S, Ao L Z and Cui G. 1988. The Duobaoshan porphyry copper deposit[M]. Beijing: Geological Publishing House. 334p (in Chinese with English abstract).
- Fu Y L. 2010. The metallogenetic prediction of the Tongshan copper deposit in Heihe city, Heilongjiang Province[D]. Master Dissertation (Jilin University), 73p (in Chinese with English abstract).
- Ge W C, Wu F Y, Zhou C Y and Abdel Rahman A A. 2005. Emplacement age of the Tahe granite and its constraints on the tectonic nature of the Ergun block in the northern part of the Great Xing'an Range[J]. *Chinese Science Bulletin*, 50: 2097-2105.
- Ge W C, Wu F Y, Zhou C Y and Zhang J H. 2007. Porphyry Cu-Mo deposits in the eastern Xing'an-Mongolian Orogenic Belt: Mineralization ages and their geodynamic implications[J]. *Chinese Science Bulletin*, 52 (24): 3416-3427.
- Green T H and Pearson N J. 1986. Rare-earth element partitioning between sphene and coexisting silicate liquid at high pressure and temperature [J]. *Chemical Geology*, 55(1-2): 105-119.
- Griffin W L, Pearson N J, Belousova E, Jackson S E, Van Achterbergh

- E, O'Reilly S Y and Shee S R. 2000. The Hf isotope composition of cratonic mantle: LAM-MC-ICPMS analysis of zircon megacrysts in kimberlites [J]. *Geochimica et Cosmochimica Acta*, 64: 133-147.
- Guo F, Fan W M, Li C W, Miao L C and Zhao L. 2009. Early Paleozoic subduction of the Paleo-Asian Ocean: Geochronological and geochemical evidence from the Dashizhai basalts, Inner Mongolia [J]. *Science in China Series D: Earth Sciences*, 52(7): 940-951.
- Han Z X, Xu Y Q and Zheng Q D. 2004. Metallogenetic series and evolution of significant metal and nonmetal mineral resources in Heilongjiang Province [M]. Harbin: Heilongjiang People's Publishing House. 241p (in Chinese with English abstract).
- Hart S R. 1988. Heterogeneousmantle domains: Signatures, genesis and mixing chronologies [J]. *Earth and Planetary Science Letters*, 90: 273-296.
- Hawkesworth C J, Herdt J M, Ellam R M and McDermott F. 1991. Element fluxes associated with subduction related magmatism [J]. *Philosophical Transactions of the Royal Society of London*, 335: 393-405.
- Heilongjiang Bureau of Geology and Mineral Resources. 1993. Detailed survey report of Tongshan copper deposit in Nenjiang city, Heilongjiang Province [R]. 221p (in Chinese).
- Hong D W, Wang S G, Xie X L, Zhang J S and Wang T. 2003. Correlation between continental crustal growth and the supercontinental cycle: Evidence form the granites with positive ϵ_{Nd} in the central Asian orogenic belt[J]. *Acta Geologica Sinica*, 77(2): 203-209 (in Chinese with English abstract).
- Hou K J, Li Y H, Zou T R, Qu X M, Shi Y R and Xie G Q. 2007. LA-MC-ICP-MS technique for Hf isotope microanalysis of zircon and its geological applications[J]. *Acta Petrologica Sinica*, 23(10): 2595-2604 (in Chinese with English abstract).
- Hou K J, Li Y H and Tian Y R. 2009. In situ U-Pb dating using laser ablation-multi ion counting-ICP-MS[J]. *Mineral Deposits*, 28(4): 481-492 (in Chinese with English abstract).
- Hou Z Q, Meng X J, Qu X M and Gao Y F. 2005. Copper ore potential of adakitic intrusives in Gangdese porphyry copper belt: Constrains from rock phase and deep melting process[J]. *Mineral Deposits*, 24(2): 108-121 (in Chinese with English abstract).
- Jian P, Liu D Y, Kröner A, Windley B F, Shi Y R, Zhang F Q, Shi G H, Miao L C, Zhang W, Zhang Q, Zhang L Q and Ren J S. 2008. Time scale of an Early to Mid-Paleozoic orogeny cycle of the long-lived Central Asian Orogenic Belt, Inner Mongolia of China: Implications for continental growth[J]. *Lithos*, 101: 233-259.
- Johnson K, Barnes C G and Miller C A. 1997. Petrology, geochemistry, and genesis of high-Al tonalite and trondhjemites of the Cornucopia stock, Blue Mountains, northeastern Oregon[J]. *Journal of Petrology*, 38: 1585-1611.
- Kay S M, Mpodozis C and Coira B. 1999. Magmatism, tectonism, and mineral deposits of the central Andes ($22^{\circ} \sim 33^{\circ}$ S)[A]. In: Skinner B J, ed. *Geology and ore deposits of the Central Andes*[C]. Society of Economic Geologist Special Publications. 7: 27-59.
- Kay S M and Mpodozis C. 2001. Central Andean ore deposits linked to evolving shallow subduction systems and thickening crust [J]. *GSA Today*, 11(3): 4-9.
- Kay S M and Mpodozis C. 2002. Magmatism as probe to the Neogene shallowing of the Nazca plate beneath the modern Chilean flatslab [J]. *Journal of South American Earth Sciences*, 15: 39-57.
- Kelemen P B, Johnson K T M, Kinzler R J and Irving A J. 1990. High-field-strength element depletions in arc basalts due to mantle-magma interaction[J]. *Nature*, 345: 521-524.
- Li J Y. 2006. Permian geodynamic setting of Northeast China and adjacent regions: Closure of the paleo-Asian Ocean and subduction of the paleo-Pacific plate[J]. *Journal of Asian Earth Sciences*, 26(3-4): 207-224.
- Li J Y, Gao L M, Sun G H, Li Y P and Wang Y B. 2007. Shuangjingzi middle Triassic syn-collisional crust-derived granite in the east Inner Mongolia and its constraint on the timing of collision between Siberian and Sino-Korean paleo-plates[J]. *Acta Petrologica Sinica*, 23(3): 565-582 (in Chinese with English abstract).
- Li Z T, Wang X J, Wang H B and Wu G. 2008. Geology of the Sankuanggou gold-bearing iron-copper deposit in Nenjiang County, Heilongjiang Province[J]. *Geology and Resources*, 17 (3): 170-174 (in Chinese with English abstract).
- Liu C, Mu Z G, Liu R X and Huang B L. 1995. $^{40}\text{Ar}/^{39}\text{Ar}$ laser microprobe dating on hydrothermal minerals form Duobaoshan porphyry copper mining district, Heilongjiang Province, China[J]. *Chinese Journal of Geology*, 30(4): 329-337 (in Chinese with English abstract).
- Liu D Y, Jian P, Zhang Q, Zhang F Q, Shi Y R, Shi G H, Zhang L Q and Tao H. 2003. SHRIMP dating of adakites in the Tulinkai ophiolite, Inner Mongolia: Evidence for the early Paleozoic subduction[J]. *Acta Geologica Sinica*, 77(3): 317-327 (in Chinese with English abstract).
- Liu H T, Zhang Q, Liu J M, Ye J, Zeng Q D and Yu C M. 2004. Adakite versus porphyry copper and epithermal gold deposits: A possible metallogenetic specialization of magmatism required in-deep assessment[J]. *Acta Petrologica Sinica*, 20(2): 205-218 (in Chinese with English abstract).

- Liu J, Wu G, Zhong W and Zhu M T. 2010. Fluid inclusion study of the Duobaoshan porphyry Cu (Mo) deposit, Heilongjiang Province, China[J]. *Acta Petrologica Sinica*, 26(5): 1450-1464 (in Chinese with English abstract).
- Liu J, Wu G, Li Y, Zhu M T and Zhong W. 2012. Re-Os sulfide (chalcopyrite, pyrite and molybdenite) systematics and fluid inclusion study of the Duobaoshan porphyry Cu (Mo) deposit, Heilongjiang Province, China[J]. *Journal of Asian Earth Sciences*, 49: 300-312.
- Liu Y F, Yang Z M, Xie Y L, Zhou P, Du D H, Li Y X, Li Q Y, Qu H C and Xu B. 2012. Zircon SHRIMP U-Pb age and geochemistry of intrusive rocks from Nongruri gold deposit, Gangdese, Tibet[J]. *Mineral Deposits*, 31(4): 727-744 (in Chinese with English abstract).
- Martin H. 1999. Adakitic magmas: Modern analogues of Archean granitoids[J]. *Lithos*, 46: 411-429.
- Miao L C, Liu D Y, Zhang F Q, Fan W M, Shi Y R and Xie H Q. 2007. Zircon SHRIMP U-Pb ages of the "Xinghuadukou Group" in Hanjiayuanzi and Xinlin areas and the "Zhalantun Group" in Inner Mongolia, Da Hinggan Mountains[J]. *Chinese Science Bulletin*, 52(8): 1112-1124.
- Muir R J, Weaver S D, Bradshaw J D, Eby G N and Evans J A. 1995. Geochemistry of the Cretaceous Separation Point Batholith, New Zealand: Granitoid magmas formed by melting of mafic lithosphere [J]. *Journal of the Geological Society London*, 152: 689-701.
- Mungall J E. 2002. Roasting the mantle: Slab melting and the genesis of major Au and Au-rich Cu deposits[J]. *Geology*, 30(10): 915-918.
- Oyarzun R, Marquez A, Lillo J, Lopez I and Rivera S. 2001. Giant versus small porphyry copper deposits of Cenozoic age in northern Chile: Adakitic versus normal calc-alkaline magmatism [J]. *Mineralium Deposita*, 36: 794-798.
- Pearce J A, Harris N B W and Tindale A G. 1984. Trace element discrimination diagrams for the tectonic interpretation of granitic rocks [J]. *Journal of Petrology*, 25: 956-983.
- Pearce J A and Peate D W. 1995. Tectonic implications of the composition of volcanic arc magmas[J]. *Annual Review of Earth and Planetary Sciences*, 23: 251-285.
- Pearce J A, Kempton P D, Nowell G M and Noble S R. 1999. Hf-Nd element and isotope perspective on the nature and provenance of mantle and subduction components in western Pacific arc-basin systems[J]. *Journal of Petrology*, 40: 1579-1611.
- Pei F P, Xu W L, Yang D B, Zhao Q G, Liu X M and Hu Z C. 2007. Zircon U-Pb geochronology of basement metamorphic rocks in the Songliao Basin[J]. *Chinese Science Bulletin*, 52 (7): 942-948.
- Petford N and Atherton M P. 1992. Granitoid emplacement and deformation along a major crustal lineament: The Cordillera Blanca, Peru [J]. *Tectonophysics*, 205: 171-185.
- Petford N and Atherton M P. 1996a. Na-rich partial melts from newly underplated basaltic crust: The Cordillera Blanca batholith, Peru [J]. *Journal of Petrology*, 37: 1491-1521.
- Petford N, Atherton M P and Halliday A N. 1996b. Rapid magma production rates, underplating and remelting in the Andes: Isotopic evidence from northern-central Peru[J]. *Journal of South American Earth Sciences*, 9: 69-78.
- Petford N and Gallagher K. 2001. Partial melting of mafic (amphibolitic) lower crust by periodic influx of basaltic magma[J]. *Earth and Planetary Science Letters*, 193: 483-499.
- Qu X M, Wang R J, Dai J J, Li Y G, Qi X, Xin H B, Song Y and Du D D. 2012. Discovery of Xiongmei porphyry copper deposit in middle segment of Bangonghu-Nujiang suture zone and its significance [J]. *Mineral Deposits*, 31(1): 1-12 (in Chinese with English abstract).
- Rabbia O M, Reich M, Hernandez L B, King R W and Lopez-Escobar L. 2000. High-Al TTG-like suite at the El Teniente porphyry copper deposit, Chile[J]. 9th Congreso Geologico Chileno Puerto Varas, Abstr. 1: 326-330.
- Reich M, Parada M A, Palacios C, Dietrich A, Schultz F and Lehmann B. 2003. Adakite-like signature of Late Miocene intrusions at the Los Pelambres giant porphyry copper deposit in the Andes of central Chile: Metallogenetic implications[J]. *Mineralium Deposita*, 38: 876-885.
- Rui Z Y, Zhang H T, Chen R Y, Wang Z L, Wang L S and Wang Y T. 2006. An approach to some problems of porphyry copper deposits[J]. *Mineral Deposits*, 25(4): 491-500 (in Chinese with English abstract).
- Sajona F G and Maury R C. 1998. Association of adakites with gold and copper mineralization in Philippines. *Comptes rendus de l'Académie des sciences. Série II, Sciences de la terre et des planètes* [J]. *Earth and Planetary Sciences*, 326: 27-34.
- She H Q, Li J W, Xiang A P, Guan J D, Yang Y C, Zhang D Q, Tan G and Zhang B. 2012. U-Pb ages of the zircons from primary rocks in middle-northern Daxinganling and its implications to geotectonic evolution[J]. *Acta Petrologica Sinica*, 28(2): 571-594 (in Chinese with English abstract).
- Shi G H, Liu D Y, Zhang F Q, Jian P, Miao L C, Shi Y R and Tao H. 2003. Zircon SHRIMP U-Pb geochronology and significance of the Xilinhot metamorphic complex, Inner Mongolia, China[J]. *Chinese Science Bulletin*, 48(4): 2187-2192 (in Chinese).

- Shi Y R, Liu D Y, Zhang Q, Jian P, Zhang F Q, Miao L C, Shi G H, Zhang L Q and Tao H. 2004. SHRIMP dating of diorites and granites in southern Suzuoqi, Inner Mongolia[J]. *Acta Geologica Sinica*, 78(6): 789-799 (in Chinese with English abstract).
- Smithies R H. 2000. The Archean tonalite-trondhjemite-granodiorite (TTG) series is not an analogue of Cenozoic adakite[J]. *Earth and Planetary Science Letters*, 82: 115-125.
- Soderlund U, Patchett P J, Vervoort J D and Isachsen C E. 2004. The ^{176}Lu decay constant determined by Lu-Hf and U-Pb isotope systematics of Precambrian mafic intrusions[J]. *Earth and Planetary Science Letters*, 219: 311-324.
- Stern R J. 2002. Subduction zones[J]. *Reviews of Geophysics*, 40: 1-38.
- Sui Z M, Ge W C, Wu F Y, Zhang J H, Xu X C and Cheng R Y. 2007. Zircon U-Pb ages, geochemistry and its petrogenesis of Jurassic granites in northeastern part of the Da Hinggan Mountains[J]. *Acta Petrologica Sinica*, 23(2): 461-480 (in Chinese with English abstract).
- Sun D Y, Wu F Y and Gao S. 2004. LA-ICP-MS zircon U-Pb age of the Qingshui pluton in the east Xiao Hinggan Mountains[J]. *Acta Geoscientica Sinica*, 25(2): 213-218 (in Chinese with English abstract).
- Sun D Y, Wu F Y, Gao S and Lu X P. 2005. Confirmation of two episodes of A-type granite emplacement during Late Triassic and Early Jurassic in the central Jilin Province, and their constraints on the structural pattern of Eastern Jilin-Heilongjiang area, China[J]. *Earth Science Frontiers*, 12(2): 263-275 (in Chinese with English abstract).
- Tan C Y, Wang G H and Li Y S. 2010. New progress and significance on the mineral exploration in Duobaoshan mineralization area, Heilongjiang, China[J]. *Geological Bulletin of China*, 29(2-3): 436-445 (in Chinese with English abstract).
- Taylor S R and McLennan S M. 1985. The continental crust: Its composition and evolution[M]. Oxford: Blackwell Scientific Publications, 54-374.
- Thiéblemont D, Stein G and Lescuyer J L. 1997. Gisements épithermaux et porphyriques: la connexion adakite: Comptes rendus de l'Académie des sciences. Sciences de la terre et des planètes[J]. *Earth and Planetary Sciences*, 325: 103-109.
- Vervoort J D, Pachelt P J, Gehrels G E and Nutman A P. 1996. Constraints on early Earth differentiation from hafnium and neodymium isotopes[J]. *Nature*, 379: 624-627.
- Wang G W and Huang L. 2012. 3D geological modeling for mineral resource assessment of the Tongshan Cu deposit, Heilongjiang Province, China[J]. *Geoscience Frontiers*, 3(4): 483-491.
- Wang J R, Jia Z L, Li T D, Ma J L, Zhao L, He Y B, Zhang W and Liu K X. 2013. Discovery of Early Devonian adakite in West Junggar, Xinjiang: Implications for geotectonics and Cu mineralization [J]. *Acta Petrologica Sinica*, 29(3): 840-852 (in Chinese with English abstract).
- Wang Q, Xu J F and Zhao Z H. 2003. Intermediate-acid igneous rocks strongly depleted in heavy rare earth elements (or adakitic rocks) and copper-gold metallogenesis[J]. *Earth Science Frontiers*, 10(4): 561-572 (in Chinese with English abstract).
- Wang Q, Tang G J, Jia X H, Zi F, Jiang Z Q, Xu J F and Zhao Z H. 2008. The metalliferous mineralization associated with adakitic rocks[J]. *Geological Journal of China Universities*, 14(3): 350-364 (in Chinese with English abstract).
- Wang X C, Liu Y S and Liu X M. 2006. Mesozoic adakites in the Linglong Basin of central North China Craton: Partial melting of underplated basaltic lower crust[J]. *Geochemical Journal*, 40: 447-461.
- Wang X C, Wang X L, Wang L, Liu J Y, Xia B, Deng J and Xu X M. 2007. Metallogenesis and reformation of the Duobaoshan superlarge porphyry copper deposit in Heilongjiang[J]. *Chinese Journal of Geology*, 42(1): 124-133 (in Chinese with English abstract).
- Woodhead J, Eggins S and Gamble J. 1993. High field strength and transition element systematics in island and back-arc basin basalts: Evidence for multi-phase extraction and a depleted mantle wedge [J]. *Earth and Planetary Science Letters*, 114: 491-504.
- Wu F Y, Li X H, Zheng Y F and Gao S. 2007. Lu-Hf isotopic systematics and their applications in petrology[J]. *Acta Petrologica Sinica*, 23(2): 185-220 (in Chinese with English abstract).
- Wu G, Chen Y J, Sun F Y, Li J C, Li Z T and Wang X J. 2008. Geochemistry of the Late Jurassic granitoids in the northern end area of Da Hinggan Mountains and their geological and prospecting implications[J]. *Acta Petrologica Sinica*, 24(4): 899-910 (in Chinese with English abstract).
- Wu G, Liu J, Zhong W, Zhu M T, Mei M and Wan Q. 2009. Fluid inclusion study of the Tongshan porphyry copper deposit, Heilongjiang Province, China[J]. *Acta Petrologica Sinica*, 25(11): 2995-3006 (in Chinese with English abstract).
- Wu T R, He G Q and Zhang C. 1998. On Palaeozoic tectonics in the Alxa region, Inner Mongolia, China[J]. *Acta Geologica Sinica*, 72(3): 256-263.
- Xie J C, Chen S, Sun W D and Yang X Y. 2012. Geochemistry of Early Cretaceous adakitic rocks in Tongling region of Anhui Province: Constraints for rock- and ore-forming[J]. *Acta Petrologica Sinica*, 28(10): 3181-3196 (in Chinese with English abstract).

- Xiang A P, Yang Y C, Li G T, She H Q, Guan J D, Li Y W and Guo Z J. 2012. Diagenetic and metallogenic ages of Duobaoshan porphyry Cu-Mo deposit in Heilongjiang Province[J]. Mineral Deposits, 31(6): 1237-1248 (in Chinese with English abstract).
- Xiong X L, Li X H, Xu J F, Li W X, Zhao Z H, Wang Q and Chen X M. 2003. Extremely high-Na adakite-like magmas derived from alkali-rich basaltic underplate: the Late Cretaceous Zhangtang andesites in the Huichang Basin, SE China[J]. Geochemical Journal, 37: 233-252.
- Xu B and Chen B. 1997. The structure and evolution of a Middle Paleozoic orogenic belt between the North China and Siberian Blocks, northern Inner Mongolia, China[J]. Science in China (Series D), 27(3): 227-232 (in Chinese).
- Xu J F, Shinjo R, Defant M J, Wang Q and Papp R P. 2002. Origin of Mesozoic adakitic intrusive rock in the Ningzhen area of east China: Partial melting of delaminated lower continental crust[J]? Geology, 30(12): 1111-1114.
- Zartman R E and Doe B R. 1981. Plumbotectonics-the model [J]. Tectonophysics, 75: 135-162.
- Zeng Q D, Liu J M, Chu S X, Wang Y B, Sun Y, Duan X X, Zhou L L and Qu W J. 2014. Re-Os and U-Pb geochronology of the Duobaoshan porphyry Cu-Mo-(Au) deposit, northeast China, and its geological significance[J]. Journal of Asian Earth Sciences, 79: 895-909.
- Zhang Q, Qin K Z, Wang Y L, Zhang F Q, Liu H T and Wang Y. 2004. Study on adakite broadened to challenge the Cu and Au exploration in China[J]. Acta Petrologica Sinica, 20(2): 195-204 (in Chinese with English abstract).
- Zhao Y M, Bi C S, Zou X Q, Sun Y L, Du A D and Zhao Y M. 1997a. The Re-Os isotopic age of molybdenite from Duobaoshan and Tongshan porphyry copper (molybdenum) deposits[J]. Acta Geoscientia Sinica, 18 (1): 61-67 (in Chinese with English abstract).
- Zhao Y M and Zhang D Q. 1997b. Metallogeny and prospective evaluations of copper-polymetallic deposits in the Great Hinggan Range and its adjacent regions[M]. Beijing: Seismological Press, 318p (in Chinese with English abstract).
- Zhao Y Y, Ma Z H and Zhong C X. 1995. Geochemistry and its model of prospecting of Tongshan copper deposit, Heilongjiang Province [J]. Geology and Prospecting, 31(3): 48-54 (in Chinese with English abstract).
- Zhao Y Y, Wang J P, Zhao G J and Cui Y B. 2011. Metallogenic regularity and prospecting direction of Duobaoshan ore field, Heilongjiang Province, China[J]. Journal of Jilin University (Earth Science Edition), 41(6): 1676-1688 (in Chinese with English abstract).
- stract).
- Zhou M F, Lesher C M, Yang Z X, Li J W and Sun M. 2004. Geochemistry and petrogenesis of 270 Ma Ni-Cu-(PGE) sulfide-bearing mafic intrusions in the Huangshan district, Eastern Xinjiang, Northwest China: Implications for the tectonic evolution of the Central Asian orogenic belt[J]. Chemical Geology, 209: 233-257.
- ### 附中文参考文献
- 曹康,许继峰,陈建林,黄肖潇,任江波. 2014. 云南普朗超大型斑岩铜矿床含矿斑岩成因及其成矿意义[J]. 矿床地质, 33(2): 307-322.
- 陈希节,许志琴,孟元库,贺振宇. 2014. 冈底斯带中段中新世埃达克质岩浆作用的年代学、地球化学及 Sr-Nd-Hf 同位素制约[J]. 岩石学报, 30(8): 2253-2268.
- 第五春荣,孙勇,林慈鉴,柳小明,王洪亮. 2007. 豫西宜阳地区 TTG 质片麻岩锆石 U-Pb 定年和 Hf 同位素地质学[J]. 岩石学报, 23 (2): 253-262.
- 杜琦,赵玉明,卢秉刚,马德友,李佩兰,律景凯,李文深,敖立志,崔革. 1988. 多宝山斑岩铜矿床[M]. 北京: 地质出版社, 334 页.
- 付艳丽. 2010. 黑龙江省黑河市铜山铜矿床成矿预测[D]. 吉林大学硕士学位论文. 73 页.
- 韩振新,徐衍强,郑庆道. 2004. 黑龙江省重要金属和非金属矿产的成矿系列及其演化[M]. 哈尔滨: 黑龙江人民出版社, 241 页.
- 黑龙江省地质矿产局. 1993. 黑龙江省嫩江县铜山铜矿详查报告 [R]. 221 页.
- 洪大卫,王式洸,谢锡林,张季生,王涛. 2003. 从中亚正 ϵ_{Nd} 值花岗岩看超大陆演化和大陆地壳生长的关系[J]. 地质学报, 77(2): 203-209.
- 侯可军,李延河,邹天人,曲晓明,石玉若,谢桂青. 2007. LA-MC-ICP-MS 锆石 Hf 同位素的分析方法及地质应用[J]. 岩石学报, 23(10): 2595-2604.
- 侯可军,李延河,田有荣. 2009. LA-MC-ICP-MS 锆石微区原位 U-Pb 定年技术[J]. 矿床地质, 28(4): 481-492.
- 侯增谦,孟祥金,曲晓明,高永丰. 2005. 西藏冈底斯斑岩铜矿带埃达克质斑岩含矿性: 源岩相变及深部过程约束[J]. 矿床地质, 24 (2): 108-121.
- 李锦轶,高立明,孙桂华,李亚萍,王彦斌. 2007. 内蒙古东部双井子中三叠世同碰撞壳源花岗岩的确定及其对西伯利亚与中朝古板块碰撞时限的约束[J]. 岩石学报, 23(3): 565-582.
- 李之彤,王希今,王宏博,武广. 2008. 黑龙江省嫩江县三矿沟含金铁铜矿床地质特征[J]. 地质与资源, 17(3): 170-174.
- 刘驰,穆治国,刘如羲,黄宝玲. 1995. 多宝山斑岩铜矿区水热蚀变矿物的激光显微探针 $^{40}\text{Ar}/^{39}\text{Ar}$ 定年[J]. 地质科学, 30(4): 329-

- 337.
- 刘敦一, 简平, 张旗, 张福勤, 石玉若, 施光海, 张履桥, 陶华. 2003. 内蒙古图林凯蛇绿岩中埃达克岩 SHRIMP 测年: 早古生代洋壳消减的证据[J]. 地质学报, 77(3): 317-327.
- 刘红涛, 张旗, 刘建明, 叶杰, 曾庆栋, 于昌明. 2004. 埃达克岩与 Cu-Au 成矿作用: 有待深入研究的岩浆成矿关系[J]. 岩石学报, 20(2): 205-218.
- 刘军, 武广, 钟伟, 朱明田. 2010. 黑龙江省多宝山斑岩型铜(钼)矿床成矿流体特征及演化[J]. 岩石学报, 26(5): 1450-1464.
- 刘云飞, 杨志明, 谢玉玲, 周平, 杜等虎, 李应栩, 李秋耘, 曲焕春, 许博. 2012. 西藏弄如日金矿床侵入岩锆石 SHRIMPU-Pb 年龄与地球化学特征[J]. 矿床地质, 31(4): 727-744.
- 曲晓明, 王瑞江, 代晶晶, 李佑国, 戚迅, 辛洪波, 宋杨, 杜德道. 2012. 西藏班公湖-怒江缝合带中段雄梅斑岩铜矿的发现及意义[J]. 矿床地质, 31(1): 1-12.
- 芮宗瑶, 张洪涛, 陈仁义, 王志良, 王龙生, 王义天. 2006. 斑岩铜矿研究中若干问题探讨[J]. 矿床地质, 25(4): 491-500.
- 余宏全, 李进文, 向安平, 关继东, 杨郎城, 张德全, 谭刚, 张斌. 2012. 大兴安岭中北段原岩锆石 U-Pb 测年及其与区域构造演化关系[J]. 岩石学报, 28(2): 571-594.
- 施光海, 刘敦一, 张福勤, 简平, 苗来成, 石玉若, 陶华. 2003. 中国内蒙古锡林郭勒杂岩 SHRIMP 锆石 U-Pb 年代学及意义[J]. 科学通报, 48(20): 2187-2192.
- 石玉若, 刘敦一, 张旗, 简平, 张福勤, 苗来成, 施光海, 张履桥, 陶华. 2004. 内蒙古苏左旗地区闪长-花岗岩类 SHRIMP 年代学[J]. 地质学报, 78(6): 789-799.
- 隋振民, 葛文春, 吴福元, 张吉衡, 徐学纯, 程瑞玉. 2007. 大兴安岭东北部侏罗纪花岗质岩石的锆石 U-Pb 年龄、地球化学特征及成因[J]. 岩石学报, 23(2): 461-480.
- 孙德有, 吴福元, 高山. 2004. 小兴安岭东部清水岩体的锆石激光探针 U-Pb 年龄测定[J]. 地球学报, 25(2): 213-218.
- 孙德有, 吴福元, 高山, 路孝平. 2005. 吉林中部晚三叠世和早侏罗世两期铅质 A 型花岗岩的厘定及对吉黑东部构造格局的制约[J]. 地学前缘, 12(2): 263-275.
- 谭成印, 王根厚, 李永胜. 2010. 黑龙江多宝山成矿区找矿新进展及其地质意义[J]. 地质通报, 29(2-3): 436-445.
- 王金荣, 贾志磊, 李泰德, 马锦龙, 赵磊, 何彦彬, 张伟, 刘昆鑫. 2013. 新疆西准噶尔发现早泥盆世埃达克岩: 大地构造及成矿意义[J]. 岩石学报, 29(3): 840-852.
- 王强, 许继峰, 赵振华. 2003. 强烈亏损重稀土元素的中酸性火成岩(或埃达克质岩)与 Cu, Au 成矿作用[J]. 地学前缘, 10(4): 561-572.
- 王强, 唐功建, 贾小辉, 资锋, 姜子琦, 许继峰, 赵振华. 2008. 埃达克质岩的金属成矿作用[J]. 高校地质学报, 14(3): 350-364.
- 王喜臣, 王训练, 王琳, 刘金英, 夏斌, 邓军, 徐秀梅. 2007. 黑龙江多宝山超大型斑岩铜矿的成矿作用和后期改造[J]. 地质科学, 42(1): 124-133.
- 吴福元, 李献华, 郑永飞, 高山. 2007. Lu-Hf 同位素体系及其岩石学应用[J]. 岩石学报, 23(2): 185-220.
- 武广, 陈衍景, 孙丰月, 李景春, 李之彤, 王希今. 2008. 大兴安岭北端晚侏罗世花岗岩类地球化学及其地质和找矿意义[J]. 岩石学报, 24(4): 899-910.
- 武广, 刘军, 钟伟, 朱明田, 麋梅, 万秋. 2009. 黑龙江省铜山斑岩铜矿床流体包裹体研究[J]. 岩石学报, 25(11): 2995-3006.
- 谢建成, 陈思, 孙卫东, 杨晓勇. 2012. 安徽铜陵早白垩世埃达克质岩地球化学: 成岩成矿制约[J]. 岩石学报, 28(10): 3181-3196.
- 向安平, 杨郎城, 李贵涛, 余宏全, 关继东, 李进文, 郭志军. 2012. 黑龙江多宝山斑岩 Cu-Mo 矿床成岩成矿时代研究[J]. 矿床地质, 31(6): 1237-1248.
- 徐备, 陈斌. 1997. 内蒙古北部华北板块与西伯利亚板块之间中古生代造山带的结构及演化[J]. 中国科学(D辑), 27(3): 227-232.
- 张旗, 秦克章, 王元龙, 张福勤, 刘红涛, 王焰. 2004. 加强埃达克岩研究, 开创中国 Cu, Au 等找矿工作的新局面[J]. 岩石学报, 20(2): 195-204.
- 赵一鸣, 毕承思, 邹晓秋, 孙亚莉, 杜安道, 赵玉明. 1997a. 黑龙江多宝山、铜山大型斑岩铜(钼)矿床中辉钼矿的铼-锇同位素年龄[J]. 地球学报, 18(1): 61-67.
- 赵一鸣, 张德全. 1997b. 大兴安岭及其邻区铜多金属矿床成矿规律与远景评价[M]. 北京: 地震出版社. 318 页.
- 赵元艺, 马志红, 仲崇学. 1995. 黑龙江铜山铜矿床地球化学及其找矿模型[J]. 地质与勘探, 31(3): 48-54.
- 赵元艺, 王江朋, 赵广江, 崔玉斌. 2011. 黑龙江多宝山矿集区成矿规律与找矿方向[J]. 吉林大学学报(地球科学版), 41(6): 1676-1688.